Working Report 2011-90

Geological Signatures of Drillhole Radar Reflectors in ONKALO

Christin Döse
Jaana Gustafsson

December 2011

POSIVA OY
Olkiluoto
FI-27160 EURAJOKI, FINLAND
Tel +358-2-8372 31
Fax +358-2-8372 3809

Working Report 2011-90

Geological Signatures of Drillhole Radar Reflectors in ONKALO

Christin Döse

Jaana Gustafsson

Tyréns AB

December 2011

Working Reports contain information on work in progress
or pending completion.

GEOLOGICAL SIGNATURES OF DRILLHOLE RADAR REFLECTORS IN ONKALO

ABSTRACT

The geological signatures of radar reflectors in ONKALO have been evaluated as a sub-activity within the Joint Work Programme "Rock Suitability Criteria – strategies and methodology" between Svensk Kärnbränslehantering AB and Posiva Oy. In addition to the geological signature, the usage of geophysical data to predict large fractures was evaluated.

Pilot hole radar loggings were carried out using a RAMAC GPR-250 MHz dipole antenna. The radar data were evaluated and reflectors with known position and intersection angle to the pilot hole were correlated with fractures or foliation in the pilot hole and with Tunnel Crosscutting Fractures in the tunnel. This data served as in-data for the evaluation of the geological signatures of radar reflectors.

The result of the evaluation is not univocal. Half of the reflectors could be explained by fractures in the pilot hole, but only about 10 % of the reflectors can be explained by Tunnel Crosscutting Fractures. Of these 10 %, 2/3 can also be explained by foliation, leaving only some 3 % of the total reflectors more unambiguously correlated with Tunnel Crosscutting Fractures.

The fractures correlated with radar reflectors do not diverge much from other fractures. Fractures having intersection angles of 30˚ – 60˚ are more likely to be detected by radar relative to other. Other properties that seem to be overrepresented in fractures correlated with radar reflectors are quartz and/or graphite content, width ≥0.8 mm and higher alteration ($J_a \geq 3$), but the data is not unambiguous.

Keywords: Radar reflector, TCF, FPI, fracture, pilot hole, drill hole, correlation

REIKÄTUTKAHEIJASTAJIEN GEOLOGISET OMINAISUUDET ONKALON PILOTTIREI'ISSÄ

TIIVISTELMÄ

Tutkaheijastajien geologisia ominaispiirteitä ONKALOssa on selvitetty osana Posiva Oy:n ja Svensk Kärnbränslehantering AB:n yhteistyöprojektia ”Rock Suitability Criteria – strategies and methodology”. Lisäksi arvioitiin geofysiikan aineiston käyttöä ennustamaan isoja rakoja.

Tutkamittauksia on pilottirei’issä tehty käyttäen RAMAC GPR-250 MHz dipoli-antennia. Tutka-aineistosta on tulkittu heijastajat joille on määritelty sijainti ja leikkaus-kulma pilottireikään nähden. Heijastajia on korreloitu pilottireiässä oleviin rakoihin ja foliaatioon sekä koko tunnelin profiilia leikkaaviin ns. TCF rakoihin. Tämä aineisto oli lähtötietona tälle työlle.

Tutkaheijastajien geologisten ominaispiirteiden selvittäminen ei ole yksiselitteistä. Puolet tutkaheijastajista selittyy raoista pilottireiässä, mutta ainoastaan 10 % heijasta-jista selittyy koko tunnelin profiilia leikkaavilla raoilla. Tästä 10 %:n osajoukosta kaksi kolmasosaa voi myös selittyä foliaatiolla, jolloin ainoastaan 3 % heijastajista voidaan varmasti korreloida tunnelin profiilia leikkaaviin rakoihin.

Raot jotka on korreloitu tutkaheijastajiin eivät juurikaan eroa muista raoista. Raot joiden leikkauskulma on $30^\circ - 60^\circ$ välillä voidaan todennäköisimmin havaita reikätutkalla muun asentoisiin rakoihin nähden. Tutkaheijastajiin korreloiduissa raoissa esiintyy muita rakoja enemmän kvartsia ja/tai grafiittia, raot ovat paksumpia ($\geq$ 0.8 mm) ja ne ovat enemmän muuttuneita ($J_a \geq 3$). Tässäkään tulokset eivät aina ole yksiselitteisiä.

Avainsanat: tutkaheijastaja, TCF, FPI, rako, pilottireikä, kairanreikä, korrelaatio

TABLE OF CONTENTS

Terminology

Large fracture	Generally, fractures that are considered significant for long term safety (might slip more than 5 cm). So far the critical fracture radius has not been defined. In practice large fractures are often equal TCF. Equal to “long fracture” which is used by SKB.
TCF	Tunnel Crosscutting Fracture. Terminology used by Posiva Oy. Equal to FPI with only a slightly different practical implementation (Hellä, 2009).
FPI	Full Perimeter Intersection. Terminology used for fractures which intersection with a tunnel can be traced around the full perimeter of a tunnel. This is a simple and uncontroversial indicator for a fracture being large (Munier, 2006). Terminology used by SKB. Equal to TCF.
Pilot hole	A drill hole that is drilled within the planned tunnel in order to study the rock properties of the area before excavation.
Alpha-angle	Intersection angle to drill hole/tunnel (0-90˚).
J_r	Joint roughness. Terminology used and defined in the Q-system for rock characterization and classification (Barton, 2002).
J_a	Joint alteration. Terminology used and defined in the Q-system for rock characterization and classification (Barton, 2002).
Ri-Class	Classification of fractured zones according to Gardemeister et al (1976). The classes are described in Table 4-4 in this report.
Radar reflector	In this report it consistently refers to pilot hole radar reflectors (dipole reflection survey).
ONKALO	Underground site characterization facility at Olkiluoto, Finland.

1 INTRODUCTION

Posiva Oy in Finland and SKB, the Swedish Nuclear Fuel and Waste Management Company, in Sweden, are both conducting a comprehensive project for the final disposal of spent nuclear fuel. The geologic disposal using a multiple barrier concept (KBS-3) has been developed in Sweden. SKB and Posiva have co-operation related to the research of the three barriers (host rock, bentonite buffer and copper canister). This work has been carried out within the co-operation project "Rock Suitability Criteria – strategies and methodology" that studies the geological, hydrological and geophysical data obtained from the underground research facility ONKALO at Olkiluoto in Eurajoki, Finland. The Swedish experience and expertise has been utilised in the work and in reviewing the results.

1.1 Background

Posiva Oy, jointly owned by Teollisuuden Voima Oyj, Fortum Power and Heat Oy, is responsible for implementing the programme for geological disposal of spent nuclear fuel in Finland. The programme consists of research, technical design and development activities, as well as construction and operation of the disposal facility. In 2000, Government made the Decision in Principle (DiP) for the disposal of spent fuel from TVO and Fortum's reactors on Olkiluoto Island in Eurajoki (Figure 1). Posiva plans to construct a KBS-3 type repository, designed to be situated at a depth of 400 m to 600 m in the bedrock at Olkiluoto. By decision of the Ministry of Trade and Industry (KTM, at present Ministry of Employment and Economy, TEM) made in 2003, Posiva is to submit an application to obtain a construction license for the disposal facility by the end of 2012.

Nuclear power companies in Sweden jointly established the Swedish Nuclear Fuel and Waste Management Company (SKB) in the 1970s. SKB’s assignment is to manage and dispose of all radioactive waste from Swedish nuclear power plants in a way to secure maximum safety for human beings and the environment. The facilities SKB is responsible for include a central interim storage facility for spent nuclear fuel (Clab) near Oskarshamn, and a final repository for short-lived radioactive waste (SFR) in Forsmark. SKB has been conducting advanced research for the final disposal of spent nuclear fuel for thirty years. A siting process was initiated 20 years ago in order to locate a potential repository for the final disposal of spent nuclear fuel. Subsequent analyses and site investigations resulted in the selection of Forsmark in Östhammar municipality in 2009. In March 2011 the applications were submitted to the Swedish Radiation Safety Authority (SSM) and to the Environmental Court to build the Spent Fuel Repository in Forsmark.

1.2 Olkiluoto site

During the past two decades, various investigations have taken place at the Olkiluoto site. Currently, construction of the underground research facility ONKALO provides opportunities to carry out investigations underground. These investigations enable the collection of more detailed information of the rock at repository depth and confirmation

of site understanding obtained during previous surface-based investigations, as well as making testing and demonstration of the disposal technology possible. The avoidance of brittle deformation zones, large fractures and transmissive fractures minimise the risks for hampering the long-term safety of the KBS-3 concept.

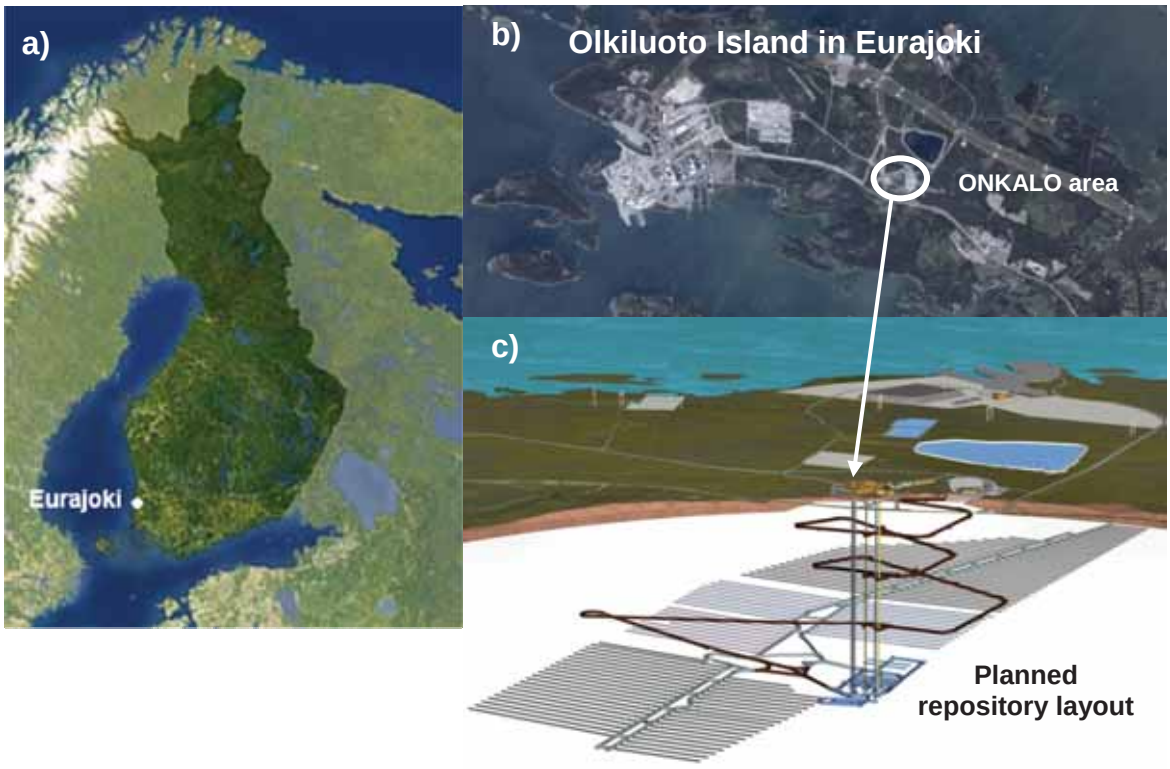

Figure 1. *a) Location of Eurajoki in western Finland. b) Olkiluoto Island and location of the ONKALO area. c) Illustration of the planned repository layout including the access tunnel, shafts and deposition tunnels at -420 m depth.*

The bedrock of Olkiluoto site area consists of Palaeoproterozoic variably migmatised gneisses and migmatites together with pegmatitic granites and diabase dikes that have been subjected to multi-phase ductile and brittle deformation during the geological history (Aaltonen et al. 2010; Lahti et al. 2009). The rocks of Olkiluoto area can be divided into four groups 1) migmatitic gneisses, 2) tonalitic-granodioritic-granitic gneisses (TGG) gneisses, 3) other gneisses including mica gneisses, quartz gneisses and mafic gneisses, and 4) pegmatitic granites (Kärki and Paulamäki 2006). Diatexitic and veined gneiss types are the most prevailing rock types in the Olkiluoto area (Fig. 2). The rock types have also been subjected to extensive hydrothermal alteration, and alteration products such as clay minerals, sulphides and illite show spatial variation in the Olkiluoto area (Aaltonen et al. 2010).

A total of 179 brittle deformation zones have been modelled in the Olkiluoto area (Aaltonen et al. 2010). These deformation zones are variable in size, but most of these zones are SE dipping. Ten hydrological zones have been modelled for the site area (Vaittinen et al. 2009). Most of these zones are prominently NE-SW orientated and some of them coincide with the modelled brittle deformation zones known in the area (Posiva Oy 2011) (Figure 3).

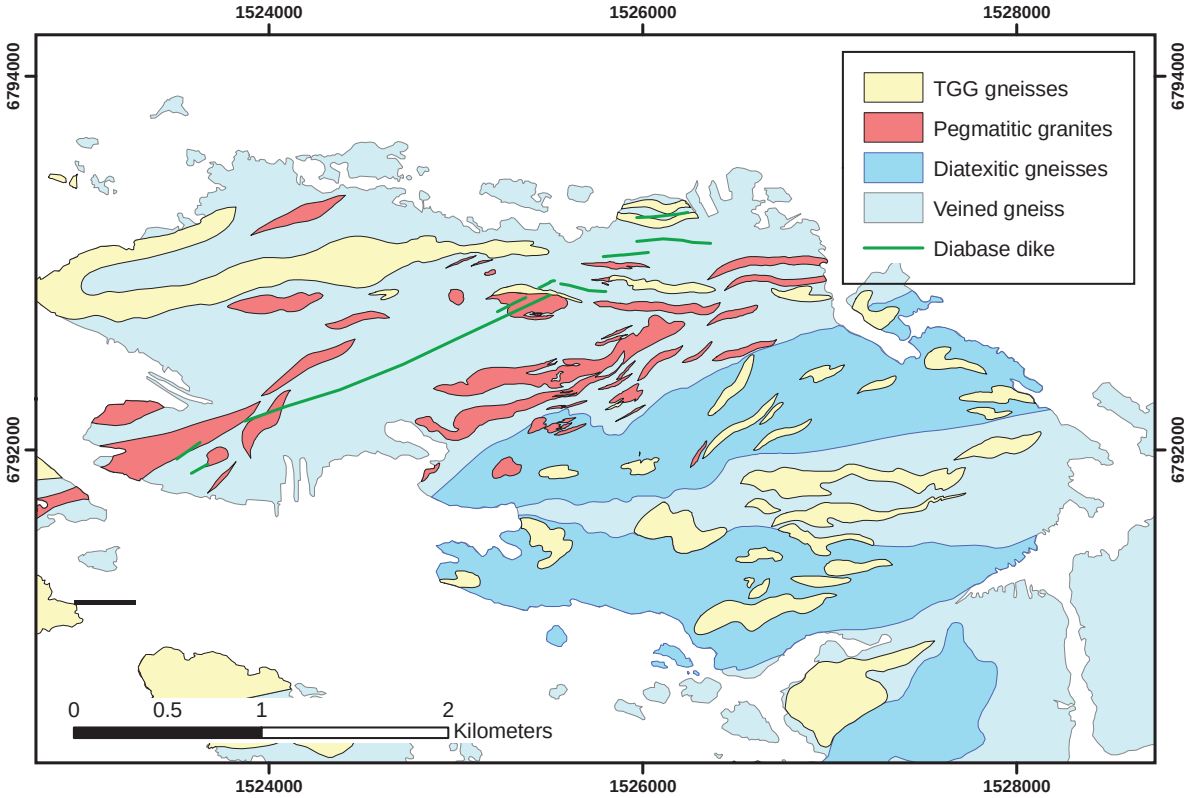

Figure 2. *A bedrock map of the Olkiluoto area.*

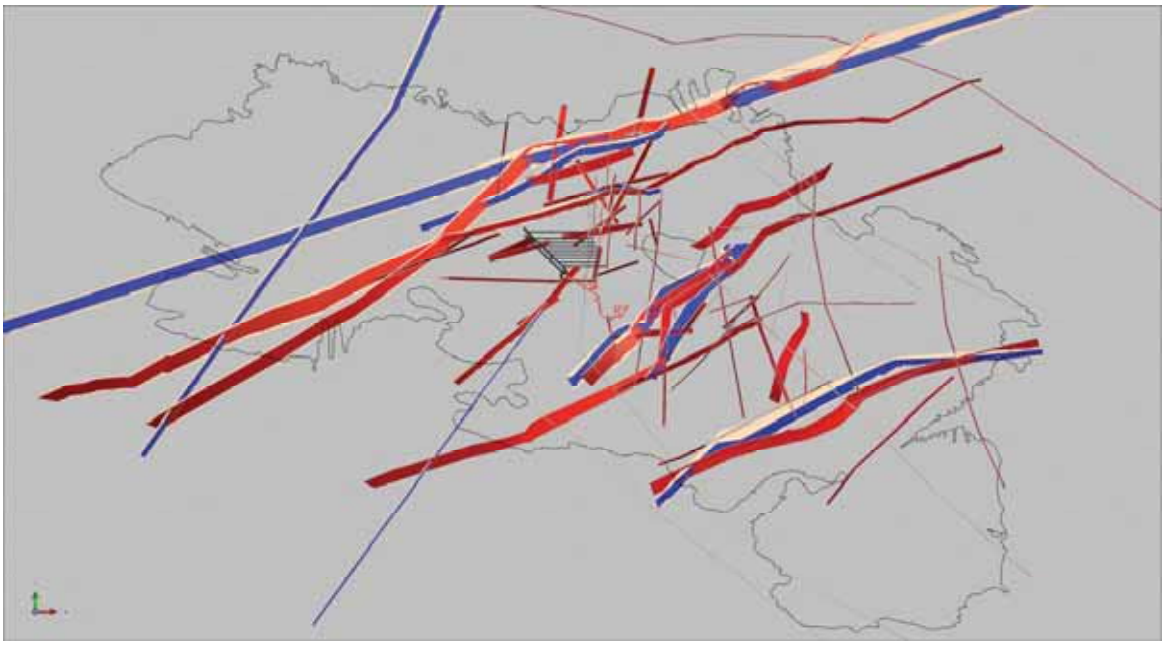

Figure 3. *Showing modelled hydrological (blue) and brittle deformation zones (red) the depth of -420 m ± 15 m. First panel together with technical rooms are also shown.*

1.3 RSC programme

In the research and development programme TKS-2006 (Posiva 2006), Posiva acknowledged the need for further development of requirements on the host rock and for ensuring their applicability and reliability of these requirements during the actual repository implementation. The Rock Suitability Criteria (RSC) programme has been set up for this purpose (Hellä et al. 2009).

The RSC-programme aims at developing a host rock classification process to be applied to the repository design and construction. This process includes determination of rock volumes suitable for the repository panels, assessment of whether deposition tunnels or tunnel sections are suitable for locating deposition holes and, finally, acceptance of each deposition hole for disposal. For this purpose, rock suitability criteria are being developed. Together with interpretation, modelling and general understanding of site properties, the criteria can be used to avoid those natural features of the host rock that may be detrimental for the safety of the repository, such as deformation zones, extensive fractures and fractures with high hydraulic conductivity.

The functionality of the RSC classification process in locating suitable rock volumes for deposition holes will be demonstrated in facilities that will be constructed in ONKALO at about -425 m level. The demonstration facilities comprise a central access tunnel, two tunnels (52 and 120 m) and a set of canister holes, which will be constructed simulating the methods and dimensions of the real deposition tunnels and holes. The demonstration will also show how the RSC-process is aligned with design and construction activities and how it functions as a part of the whole deposition process.

A detailed-scale model of the rock volume containing the planned RSC-demonstration facilities in ONKALO and parts of the planned first deposition panel will be developed simultaneously with the demonstration. The model will be constructed for the needs of the RSC and will, thus, aim at describing and predicting the rock characteristics relevant in the RSC classification process: brittle deformation zones, large fractures and inflow. The ultimate aim is to develop strategy and methodology for detailed-scale modelling of rock properties during the deposition process.

1.4 SKB-Posiva co-operation project

The ability to predict the occurrence of brittle deformation zones and single large fractures that are able to slip more than 5 cm is of great importance for the application of the RSC rock characterization process. Posiva and SKB established a co-operation project called "Rock Suitability Criteria – strategies and methodology" to develop techniques for this purpose.

The co-operation project has two objectives related to the RSC. The first objective is to develop and assess geological and geophysical investigation methods for identification of the brittle deformation zones and, especially, the large fractures. This will be carried out by analysing and correlating existing geological and geophysical data acquired from pilot holes drilled in the ONKALO access tunnel and from investigations carried out in the excavated tunnel. The second objective is to develop strategy and methodology for

creating a detailed-scale model of the rock conditions relevant to RSC, including, for example, deformation zones and large fractures.

The project comprises five activities, which are carried out using data from the ONKALO access tunnel (Figure 4):

Activity 1. The use of geological and hydrogeological data from pilot holes for predicting large fractures
Activity 2. The use of geophysical data from pilot holes for predicting large fractures
Activity 3. Suitability of seismic investigations for locating large fractures, brittle deformation zones and hydrogeological zones
Activity 4. Suitability of ground penetrating radar for locating large fractures
Activity 5. Development of strategy and methodology for detailed-scale modelling work

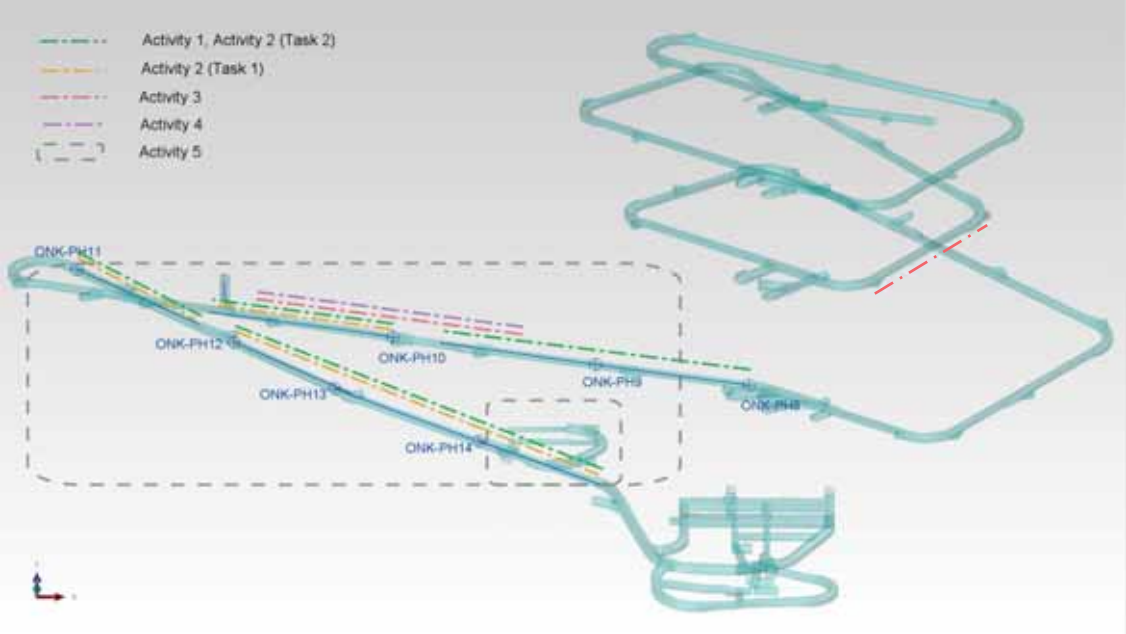

Figure 4. *Illustration of the areal coverage of activities 1-5. Locations of pilot holes ONK-PH8 to ONK-PH14 in the ONKALO access tunnel are marked.*

Activities 1 to 4 deal with data acquisition methodology. Pilot holes are the first source of direct, detailed data from a specific rock volume and it is, thus, of importance to be able to use pilot hole data in locating the relevant geologic structures. Identifying the single large fractures from a pilot hole drill core can be problematic; therefore, Activities 1 and 2 concentrate on pilot hole data and identification of large fractures. In *Activity 1*, data from the geological logging of several pilot holes from the ONKALO access tunnel are evaluated against tunnel mapping data of corresponding tunnel intervals. The purpose is to correlate tunnel cross-cutting fractures (TCF) or full perimeter intersecting fractures (FPI), (Hellä et al. 2009) with pilot hole fracture data and to determine if they have common geological characteristics. TCF is a fracture that can be observed in both walls and on the roof during the geological mapping, and FPI is a synonym for such a feature used in SKB literature (Munier 2006). It is noteworthy

that most TCFs (or FPIs) are probably not large fractures but they are considered as possible representatives of extensive features. *Activity 2* concentrates on interpretation of geophysical data obtained from pilot holes and on creating a method for using the data to predict the occurrence of the large fractures. Data on the tunnel cross-cutting fractures are used to evaluate the created method.

In Activities 3 and 4, two different geophysical methods are evaluated against the needs of the RSC-program. *Activity 3* comprises interpretation, geological correlation and evaluation of data obtained from a seismic investigation carried out in the ONKALO access tunnel with the purpose of testing the suitability of seismic investigation methods for locating local-scale geological structures, for example the large fractures. In *Activity 4*, interpretation, geological correlation and evaluation of data from ground penetrating radar investigations carried out in a research niche in ONKALO are carried out for the same purpose. Activity 5 concentrates on issues related to modelling of the acquired data and aims at developing a strategy and methodology for detailed-scale modelling of rock properties during the deposition process. This is carried out by constructing a detailed-scale model of the rock volume containing the planned RSC-demonstration facilities.

1.5 Objectives and scope of the report

The evaluation presented in this report is performed within Activity 2 of the Joint Work Programme. The objective of the evaluation is to reveal the geological properties of fractures correlated with radar reflectors, and to reveal how well large fractures are detected by radar. Are there certain fracture types that are more likely to be detected by radar or, correspondingly, some fracture types that are very unlikely to be detected by radar? Is radar logging in pilot holes a good method to predict the occurrence of large fractures?

In this work, fractures correlated with radar reflectors in pilot holes are evaluated. The evaluated data are from pilot holes ONK-PH8, ONK-PH9, ONK-PH10, ONK-PH11, ONK-PH12, ONK-PH13 and ONK-PH14, as well as the corresponding tunnel chainages 3116-4440.

1.6 Previous investigations

Special investigations have been performed earlier, where radar reflectors have been correlated with geology. Saksa et al. 2001, have correlated radar reflectors with geology in four drill holes in Olkiluoto and one drill hole in Romuvaara. Both sites are dominated by gneisses. Most radar loggings were performed with a 60 MHz antenna, but comparisons with loggings with 100 MHz and 250 MHz antennas in the same drill hole were also performed in order to sort out the radar penetration depth and radar resolution. The authors also discuss why no reflectors exist despite preferable geological conditions.

Earlier investigations performed in more homogeneous bedrock consisting of granitoids are as follows:

- Drill hole radar correlated with core mapping, Site Investigation Forsmark (Appendix in Stephens & Skagius (Editors) 2007).
- Drill hole radar correlated with core mapping, Site Investigation Oskarshamn (Carlsten 2004).
- Drill hole radar correlated with tunnel mapping, Äspö HRL (Carlsten et al. 1995, SKB, 1994 and SKB 1995.
- GPR correlated with tunnel mapping, Äspö HRL (Stenberg & Forslund 1996 and Olsson 1992).

The results from the investigations above, except for Oskarshamn data, were revisited and evaluated in greater detail in Döse & Carlsten 2011.

2 EXECUTION

2.1 In-data

In-data for the evaluation presented in this report are:

- Mapping of drill cores from pilot holes
- Radar logging in pilot holes
- Tunnel mapping
- Correlations of fractures in pilot holes with TCF in the access tunnel
- Correlation of radar reflectors with fractures in pilot holes

The in-data is described further below.

2.1.1 Investigations in pilot holes with emphasis on drill core mapping and radar logging

The geology of the oriented drill cores from the pilot hole was mapped in great detail by visual inspection. Parameters that were mapped are: lithology, foliation, fractures, fracture zones, core loss and weathering. The orientation of the geological structures are mapped both from drill cores oriented with Easy Mark and from optical image of the pilot hole.

Rock mechanical tests on the drill cores were also performed. Water conductivity measurements and chemical analysis of the groundwater were performed in the pilot holes as well as geophysical logging and optical imaging.

Results from all the investigations in pilot holes are presented in working reports. Reports of relevance to this work are listed in Table 1.

Table 1. *Information about evaluated pilot holes and tunnel sections.*

Pilot hole	Pilot hole Length (m)	Corresponding Tunnel Section (m)	Logged Radar (m)	Corresponding Tunnel Section (m)	Reference in literature (Working Reports)
ONK-PH8	150	3116-3266	143	3116-3259	Karttunen et al. 2009
ONK-PH9	150	3263-3413	145	3263-3408	Karttunen et al. 2010
ONK-PH10	180	3459-3639	149*	3459-3608	Mancini et al. 2011
ONK-PH11	131	3922-4053	129	3922-4051	Karttunen et al. 2011
ONK-PH12	124	4092-4216	122	4092-4214	Lahti et al. 2011
ONK-PH13	140	4201-4341	138	4201-4339	Aalto et al. 2011a
ONK-PH14	150	4313-4463	148	4313-4461	Aalto et al. 2011b

*The cable for radar logging is only 150 m long, which explains why the last 31 m are not logged.

Radar is one of the geophysical methods that is used in pilot holes. A drill hole radar system consists of a transmitter and a receiver antenna. During measurements an electromagnetic pulse is emitted into the bedrock. Once a structure with a different electrical property, for example a water-filled fracture, comes across, the pulse is reflected back to the receiver where it is recorded. The result from the 3D-measurements all around the pilot hole is projected into 2D and presented in the form of a radargram (Figure 5) where the position of the probes is shown along one axis and the radar wave propagation and reflection is shown along the other axis. The amplitude of the received signal is shown in the radargram with a grey scale where black and white corresponds to strong reflected signals and grey to no reflected signal. The radargram gives an image of the investigated rock, showing the geometry of plane structures (contact between layers, thin marker beds, fractures) or showing the location of limited objects around the drill hole (cavities, lenses etc.). The distance to a reflecting object or plane is determined by measuring the difference in arrival time between the direct and the reflected pulse. During interpretation of drill hole measurements point and plane reflectors are identified and their positions and intersection angles are measured using software Radinter_2.

Which antenna to use depends on the needed accuracy, resolution and penetration depth. The radar survey of the pilot holes was carried out using a RAMAC GPR-250 MHz dipole antenna. With this antenna the penetration depth is about 10 m (±5 m). The resolution is high, which means that single fractures within a zone are usually displayed in the radargrams rather than the zone itself. Using a dipole antenna, strike and dip of the radar reflectors cannot be determined; only the alpha-angle of the reflector is known. If strike and dip of the reflector are requested, a directional antenna can be used. As the authors know, directional antennas only exist as 60 MHz antennas resulting in moderate resolution.

For detailed information about radar in drill holes the reader is directed to Saksa et al. 2001 or Carlsten et al. 1995.

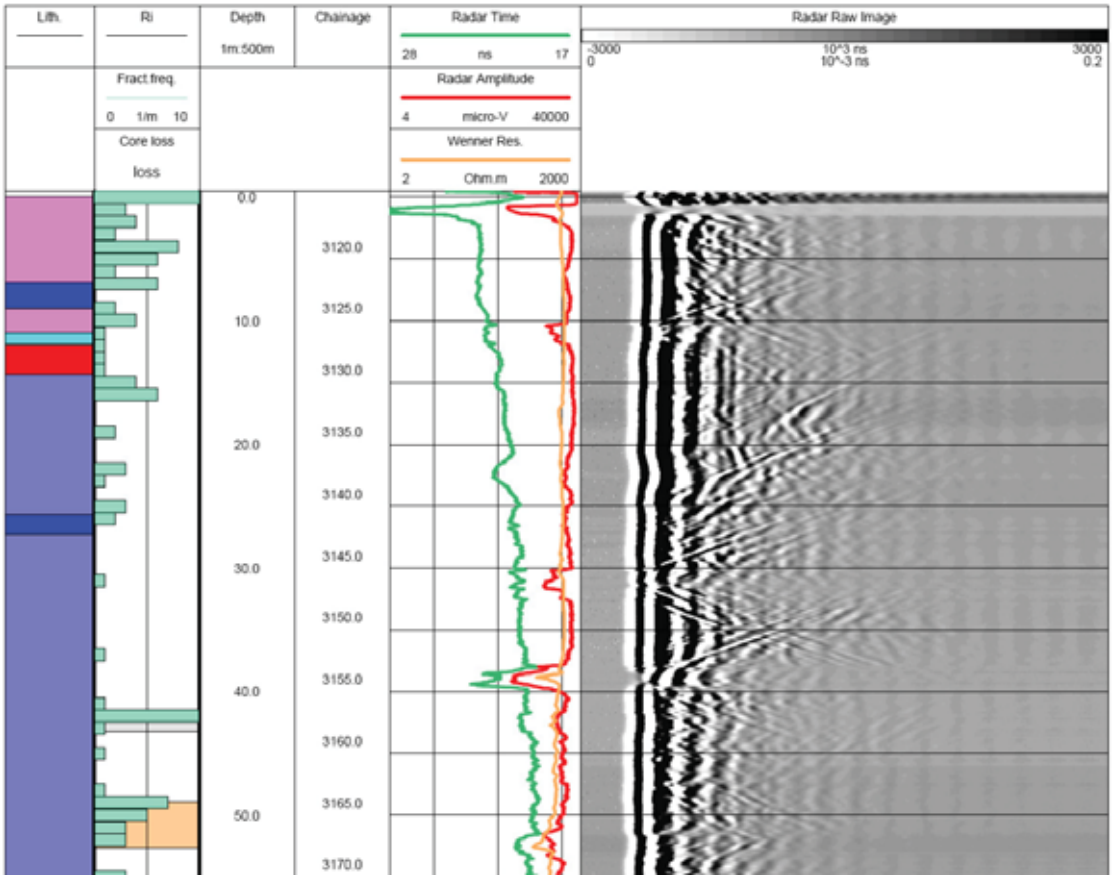

Figure 5. *Example of a radargram (to the right) presented in WellCad. Information about lithology and fracture frequencies to the left are collected during the drill core mapping (from Karttunen et al. 2009).*

2.1.2 Geological mapping of the excavated tunnel

When the tunnel was excavated the geology of the tunnel was mapped in detail, including rock type, foliation, folding and fractures and fractures zones. Fracture observations included orientation, trace length, displacement, surface morphology, filling materials, aperture, termination, undulation, water leakage and, for fractures with discernible movement, striation (Engström & Kemppainen 2008). After documentation, Tunnel Crosscutting Fractures were measured in situ with a tachymeter. These measurements were further visualised in Gemcom Surpac™ for calculating the mean orientation of the fracture.

2.1.3 Performed correlations serving as in-data

In order to find methods for predicting possible large fractures, correlations between drill core mapping, tunnel mapping and radar interpretation were executed within the Joint Work Programme between Posiva Oy and Svensk Kärnbränslehantering AB. Two separately performed correlations served as in-data for this work:

1) Correlations between mapped TCF in the access tunnel and mapped fractures in pilot holes were performed by Antti Joutsen at Posiva Oy. Position, orientation in 3D and geological properties were used as criteria in the correlation between TCF and fractures in pilot holes (Joutsen 2011).
2) Correlations between radar reflectors and pilot hole fractures were performed by Eero Heikkinen and Ida Ravimo at Pöyry. The correlations were performed by plotting the alpha- and beta-angles of fractures and foliation (i.e. relative 3D orientations) together with alpha-angles of radar reflectors (orientations in 2D) in WellCad having the pilot hole length as y-axis (Figure 6). When the positions of the reflector and the fracture were ±2m and the alpha-angles were within 20˚, the fracture was considered a possible candidate for the reflector. Of several possible fracture candidates, the one that is most likely was selected (for example if the fracture has an electrical or susceptibility anomaly, or if fracture is filled with conductive minerals, such as clay, sulphide or graphite). Correlations with foliation were usually only made if no matching fracture was found. The correlations are presented in working reports listed in Table 3-1).

An example of a fracture in the pilot hole, a TCF in the tunnel and a radar reflector that can be correlated with each other is shown in Figure 7.

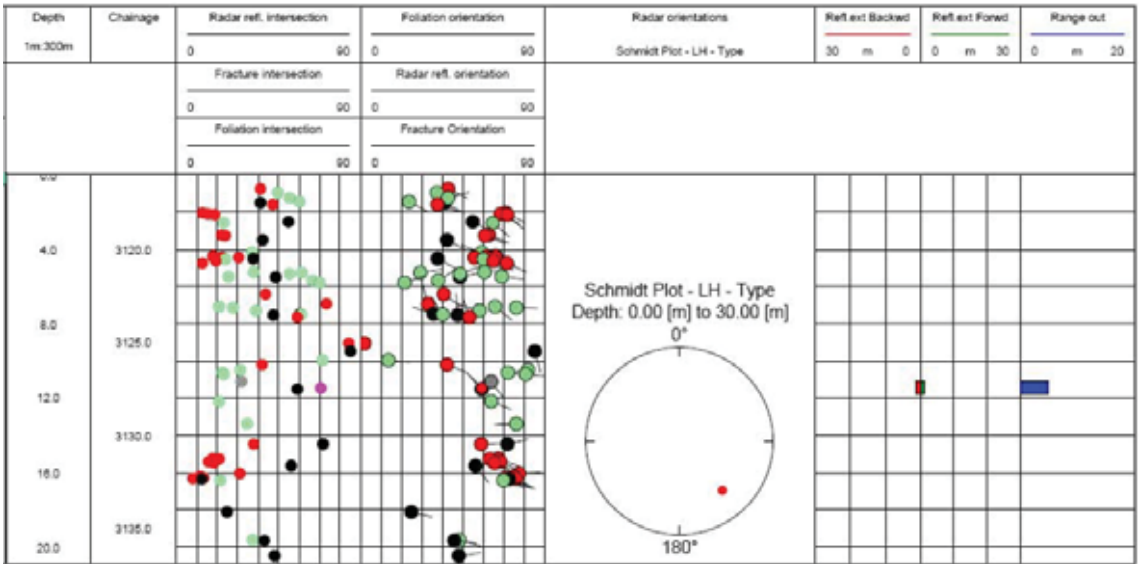

Figure 6. *Example of correlation between pilot hole fractures and radar reflectors using software WellCad (from Karttunen et al, 2009).* ● *= Radar reflector.*

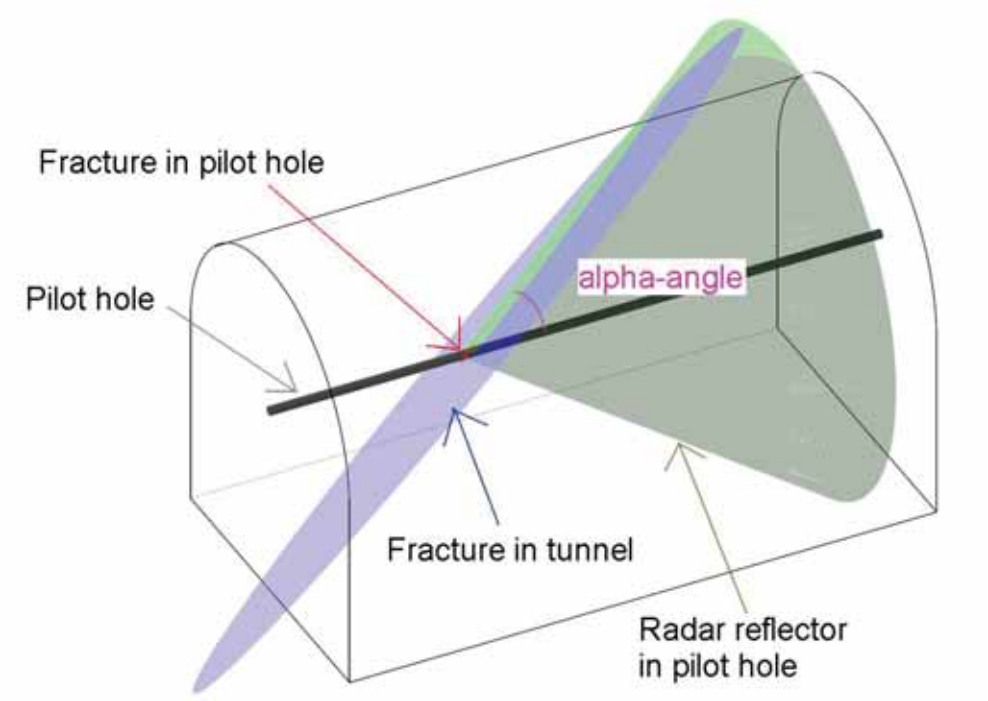

Figure 7. *Schematic figure of a pilot hole in the tunnel, where the fracture in the pilot hole, the fracture in the tunnel and the radar reflector can be correlated with each other. The 2D radar reflector is displayed as a cone along the pilot hole in 3D, since the beta-angle or rotation angle of the reflector is not known. The alpha-angle of the fracture in the pilot hole is poorly visible in this scale.*

2.2 Evaluation of data

The evaluation of data was mainly performed in tables. The tables with correlations between TCF and pilot hole fractures as well as correlations between radar reflectors and pilot hole fractures (in-data to the evaluation) were sorted, after which fracture properties were evaluated in relation to background data. During the correlation with pilot hole data, all fractures from the investigated pilot holes served as background data, whereas during the evaluation of correlated TCFs, all TCFs within the tunnel sections corresponding to pilot hole radar logging served as background data (Table 4-1). The evaluation was performed by comparing percentages of certain properties in both groups (correlated fractures and background fractures). The results of the comparisons are displayed in histograms.

In the evaluation the number of fractures in the data differs from the total number of fractures in both groups (Figures 8 – 13 and Figure 19). This is because data is missing for some fractures in the drill core mapping. When data is missing the actual fracture is excluded in the evaluation, which means that the sum of the properties displayed in a histogram is always 100 %, with one exception for fracture mineralogy that will be explained in chapter 3.

The correlations of radar reflectors with TCFs were revisited with a different approach. Instead of correlating radar reflectors with pilot hole fractures, which in turn were

correlated with TCFs, radar reflectors were correlated directly with TCFs. In order to do that, the alpha-angle of each TCF to the pilot hole (Figure 7) was calculated as well as the corresponding tunnel sections of the reflectors. After this, the position and alpha-angle of the reflector was correlated with a TCF with similar position and alpha-angle. Similar positions were considered being within ± 3m and similar alpha-angles were considered being within ± 10˚. Greater differences in position were allowed if the alpha-angle was small, whereas greater differences in alpha were allowed if the alpha-angle was >50˚). Additionally, the radargrams were studied in order to see if reflectors possibly corresponding to TCFs could have been missed in the interpretation. It was found that this was sometimes the case. However, no reinterpretations of radargrams were performed, since it was beyond the scope of this work. This is discussed further in chapter 4.

3 RESULTS

3.1 Radar reflectors correlated with fractures in pilot holes

There were 158 radar reflectors correlated with core mapping of pilot holes, of which 52 % (n=82) could be correlated with fractures (Table 2) and 37 % (n=59) were correlated with foliation. The number of correlations are not explicit, since only one candidate was generally correlated to the reflector. Many reflectors correlated with fractures could as well be correlated with foliation. As much as 8 % (n=12) of the radar reflectors do not intersect the pilot hole and could therefore not be correlated with core mapping. Finally, only 3 % (n=5) of the radar reflectors did not have any geological explanation in the core mapping data.

The mineralogy of fractures correlated with radar reflectors, relative to all fractures are shown in Figure 8. It seems that graphite, muscovite and chlorite are overrepresented among the fractures correlated with radar reflectors compared to background data, while calcite is underrepresented. The average number of fracture minerals mapped in fractures correlated with radar reflectors is 2.23 minerals/fracture, while it is 1.98 minerals/fracture for background data. This explains why the percentages of minerals are generally higher for fractures correlated with reflector relative to background.

There is no clear difference in fracture type (Figure 9) and the thickness of fracture filling (Figure 10) between fractures correlated with radar reflector relative to all fractures. Also, the joint roughness profiles of fractures correlated with reflector relative to all fractures are quite similar (Figure 11) and the clear dominance of undulated and slickensided fractures, which is typical of TCF (Figure 16), is not observable in the data. The histogram showing the joint alteration of fractures correlated with radar reflectors relative to joint alteration of all mapped fractures looks confusing, with J_a=1 (non-altered coatings) and J_a=4 (low friction coatings) overrepresented among fractures correlated with radar reflectors relative to background, while J_a=2 is underrepresented (slightly altered coatings, Figure 12).

Table 2. *Summary of results from correlation of radar reflectors with pilot hole fractures.*

Reflectors correlated with	n	%
Fractures	82	52
Foliation	59	37
No core intersection	12	8
No correlation	5	3
TOTAL	158	100

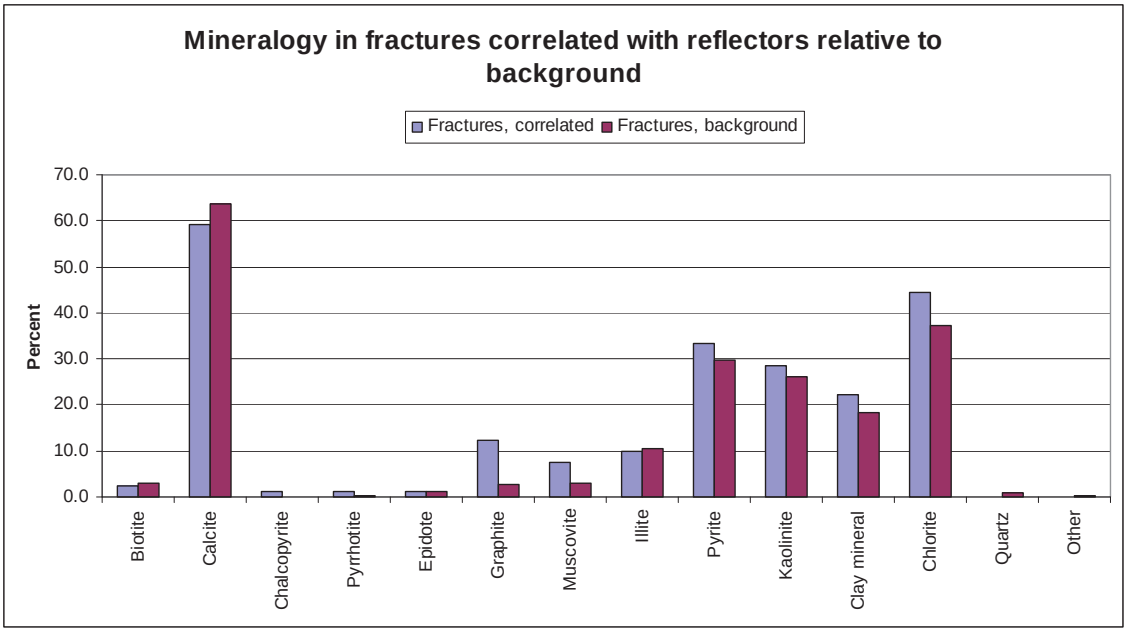

Figure 8. *Mineralogy in fractures correlated with radar reflector (n=81) compared to all fractures in pilot holes PH8-PH14 (n=1760). One fracture which was correlated with a fracture only observed in drillhole image was excluded. Note that the histogram does not take into account the amount of certain minerals in the fractures, but only the occurrence.*

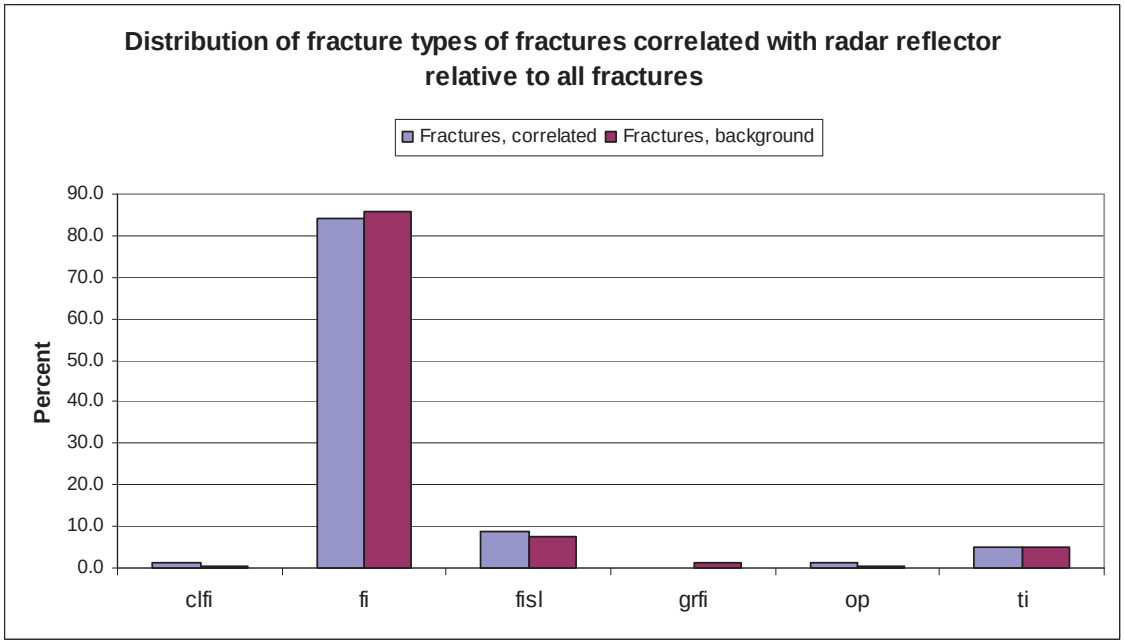

Figure 9*. Distribution of fracture types of fractures correlated with radar reflector (n=81) compared to all fractures in pilot holes PH8-PH14 (n=1699). One fracture which was correlated with a fracture only observed in drillhole image was excluded. Clfi= clay filled, fi=filled, fisl= filled and slickensided, grfi= grain filled, op=open and ti=tight.*

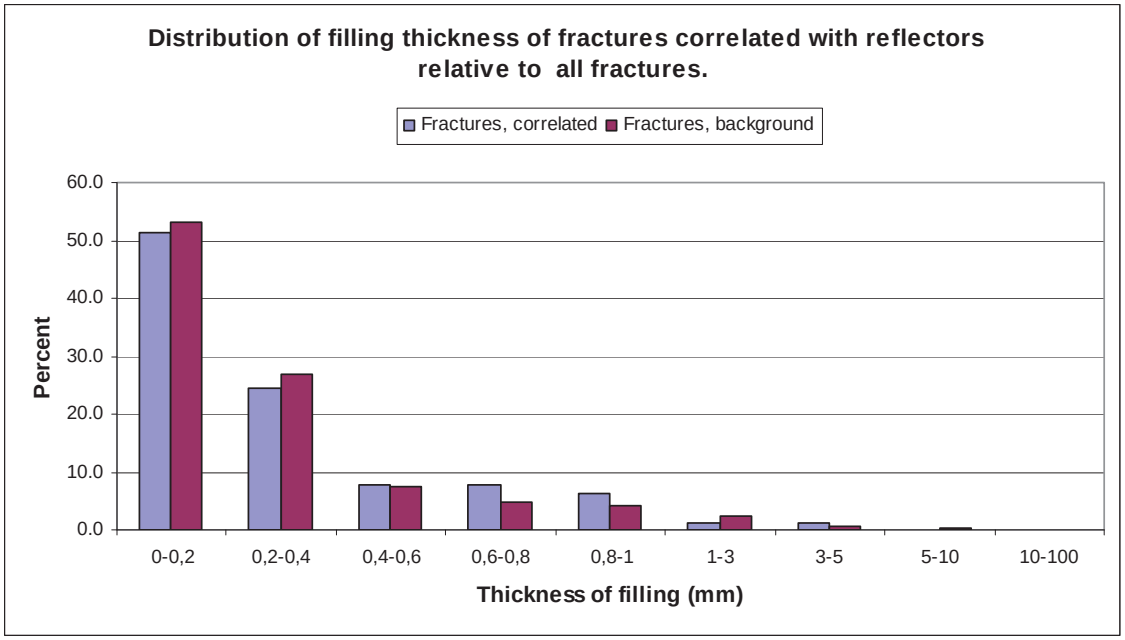

Figure 10. *Distribution of filling thickness of fractures correlated with radar reflector (n=78) compared to all fractures in pilot holes PH8-PH14 (n=1633).*

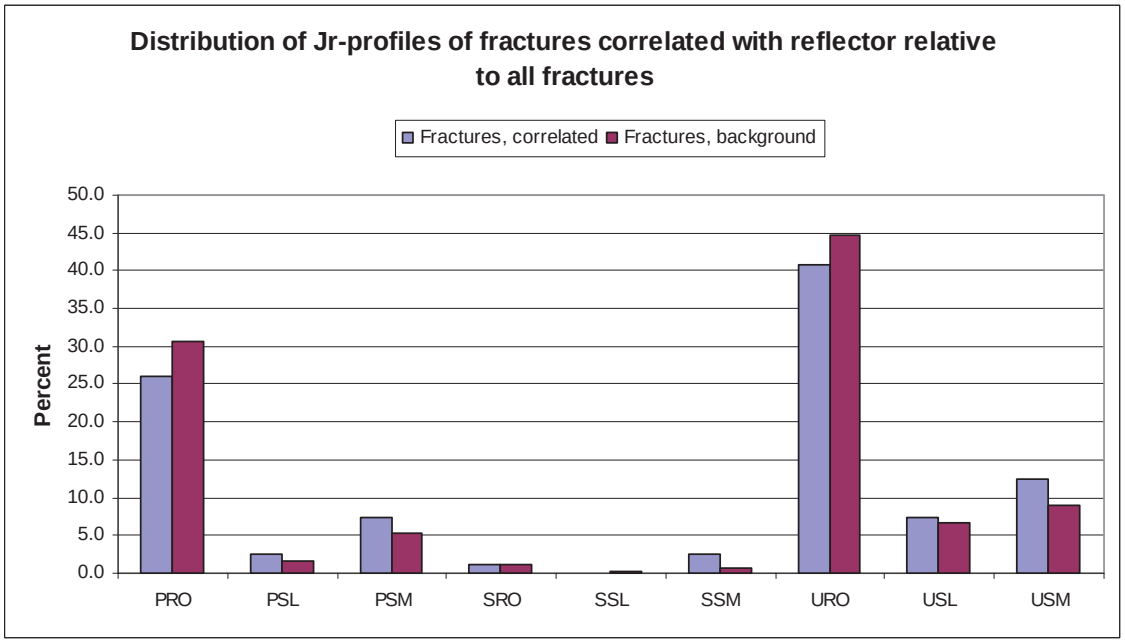

Figure 11. *Distribution of Joint roughness profiles (J_r) of fractures correlated with reflector (n=81) relative to all fractures (n=1690). PRO= Planar rough, PSL= Planar slickensided, PSM= Planar smooth, SRO= Stepped rough, SSL= Stepped slickensided, SSM= Stepped smooth, URO= Undulating rough, USL= Undulating slickensided, USM= Undulating smooth.*

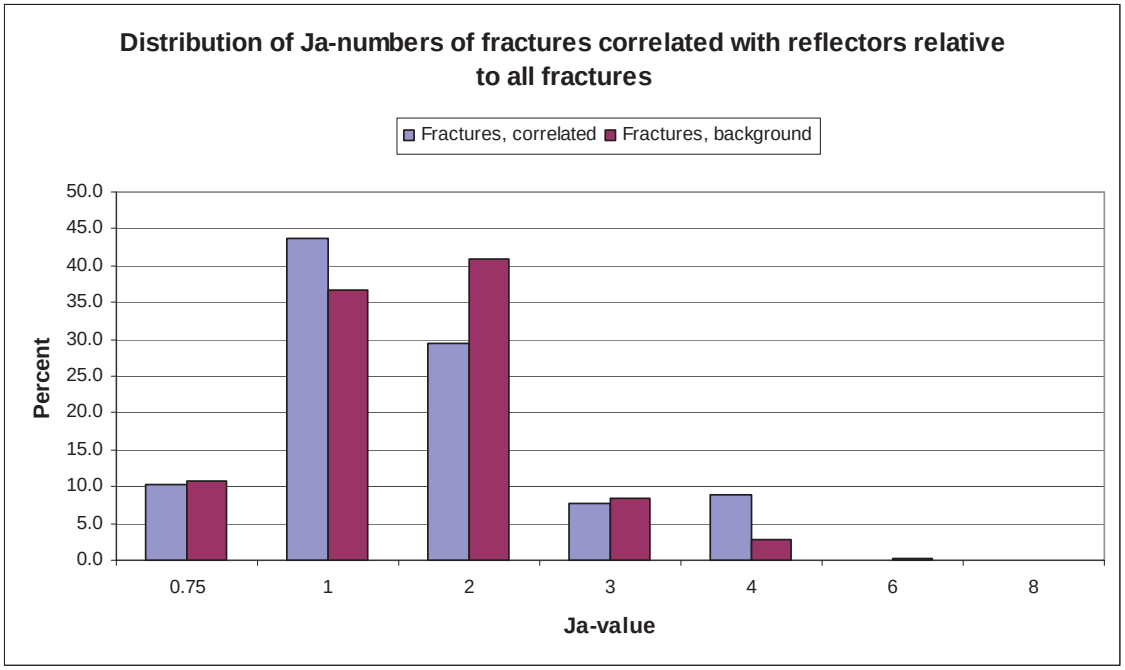

Figure 12. *Distribution of Joint alteration numbers (J_a) of fractures correlated with radar reflector (n=78) compared to all fractures in pilot holes ONK-PH8-ONK-PH14 (n=1698).*

In accordance with previous investigations (Stephens & Skagius (Editors) 2007; Carlsten 2004; Carlsten et al. 1995; SKB 1994; SKB 1995; Stenberg & Forslund 1996 and Olsson 1992), a preferable alpha-angle of a fracture is important for its detection in radargrams. Fractures having alpha-angles of 40-60˚ are clearly overrepresented among fractures correlated with radar reflectors relative to all fractures, while fractures having alpha-angles of 0-20˚ and 60-90˚ are clearly underrepresented (Figure 13). In chapter 4 the alpha-angle is discussed further.

The orientation of fractures correlated with radar reflectors varies. In some pilot holes fractures belonging to main fracture sets seem to be overrepresented among the correlated fractures, as in ONK-PH8, ONK-PH13 and ONK-PH14, but also the opposite is observed (Figures A1-1 – A1-7). In Figure A1-8 all correlated fractures are plotted together.

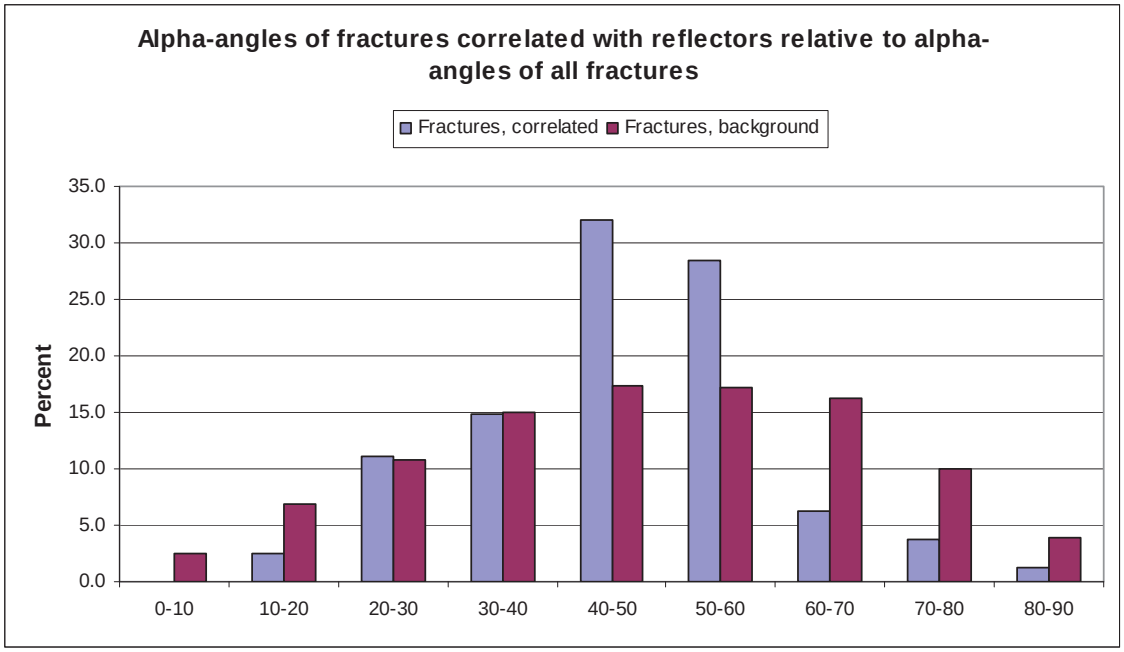

Figure 13*. Alpha-angles of fractures correlated with reflectors (n=81) relative to alpha-angles of all fractures (n=1682).*

3.2 Radar reflectors correlated with Tunnel Crosscutting Fractures (TCF)

In the received data that was to be evaluated, the 158 radar reflectors were correlated to pilot hole fractures, which in turn were correlated with TCFs. This resulted in only 3 correlations between TCFs and radar reflectors, or detection of only ~5 % of all TCFs with pilot hole radar (Table 4-2). This also inferred that only ~2 % of the reflectors were explained by TCF.

An attempt correlating the 158 radar reflectors directly with TCFs in the tunnel revealed another 17 reflectors that could be correlated with TCFs. This means that ~13 % of the reflectors could be explained by TCF. Since two of the TCFs have two possible reflectors, the amount of correlated TCFs was hereby increased to 18 or 31 % of all TCFs within the investigated tunnel sections (Table 3, Appendix 2). The reason for this may be the following:

- Greater variations between position and possibly also alpha-angle of the reflector and the TCFs were allowed.
- Candidates with other strike and dip, but with similar alpha-angle, were not excluded only because another fracture or a foliation plane had a better fit in position and alpha-angle.

Of the 20 radar reflectors correlated directly with 18 TCFs in the tunnel (two TCF have two possible reflectors), 8 were initially correlated with foliation in the pilot hole, while 11 were correlated with fractures and 1 had no correlation. Still another 4 reflectors correlated with TCFs could also be explained by foliation. This means that 2/3 of the reflectors correlated with TCFs could be explained by foliation as well.

Table 3. *Evaluation of correlating radar reflectors with pilot hole fractures which in turn are correlated with TCFs.*

Correlation	no.	% of all reflectors	Detection of all TCF-fractures (%)
Number of radar reflectors	158		
Number of TCF-fractures within investigated tunnel sections	59		
Radar reflectors that can be correlated with TCF	20	13	31*
Radar reflector, which is correlated with a pilot hole fracture, which in turn is correlated with a TCF-fracture	3	2	5
Radar reflector confidently correlated with a TCF-fracture, that also could be explained by foliation	12	8	20

** Percent is calculated from 18 detected TCF, since two TCF can be correlated to two radar reflectors.*

In this report, the 18 TCFs correlated with radar reflectors are evaluated further. It is very important to emphasize that the amount of TCFs correlated with radar reflectors is too small to make statistically valid conclusions. The histograms in this subchapter do only represent the 18 correlated TCFs within this work and do not necessarily represent general properties of TCFs causing radar reflectors.

The mineralogy of TCFs correlated with radar reflectors relative to all TCFs in the investigated tunnel sections are shown in Figure 14. It seems that quartz and graphite are overrepresented among TCFs captured by radar. Because graphite is a conductive mineral, and 75 % of the correlated TCF fractures containing quarts do also contain graphite, this result is reasonable. The average number of fracture minerals mapped in TCFs correlated with radar reflectors is 4.7 minerals/fracture, while it is 4.4 minerals/fracture for background data.

There also seems to be a slight overrepresentation of thicker fracture fillings among the TCFs that are captured by radar (Figure 15). The shape of the TCFs does not seem to play any role for its visibility in radargrams (Figure 16), while the alteration of the fracture might have some influence (Figure 17). In the histogram, a slight overrepresentation of J_a-values ≥ 3, i.e. fractures with softening or low friction fillings, among TCFs captured by radar can be observed.

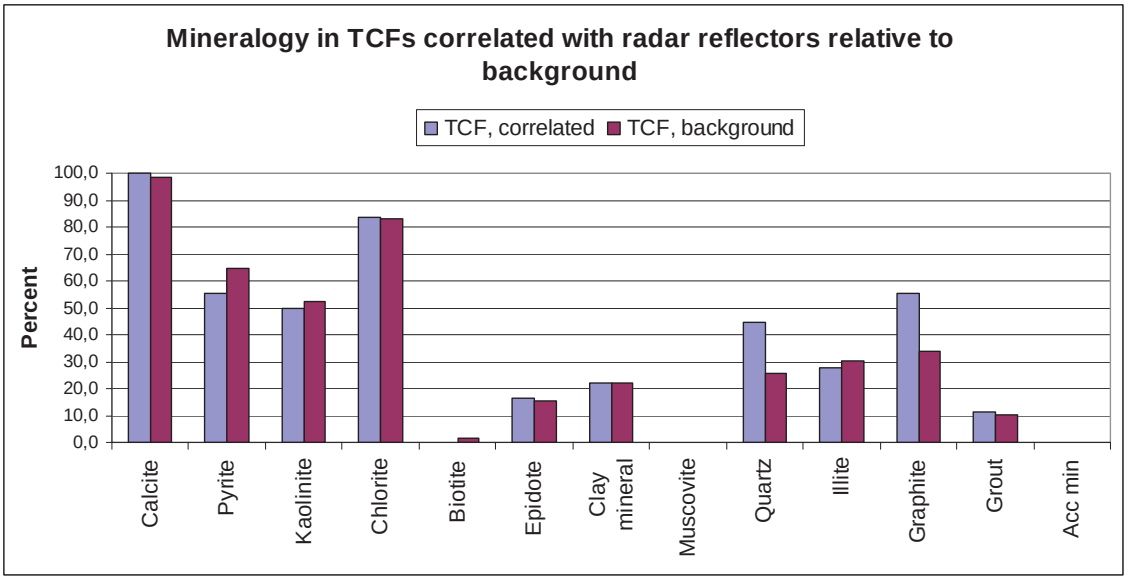

Figure 14. *Mineralogy in TCFs correlated with radar reflector (n=18) compared to all TCFs within investigated tunnel sections (n=59).*

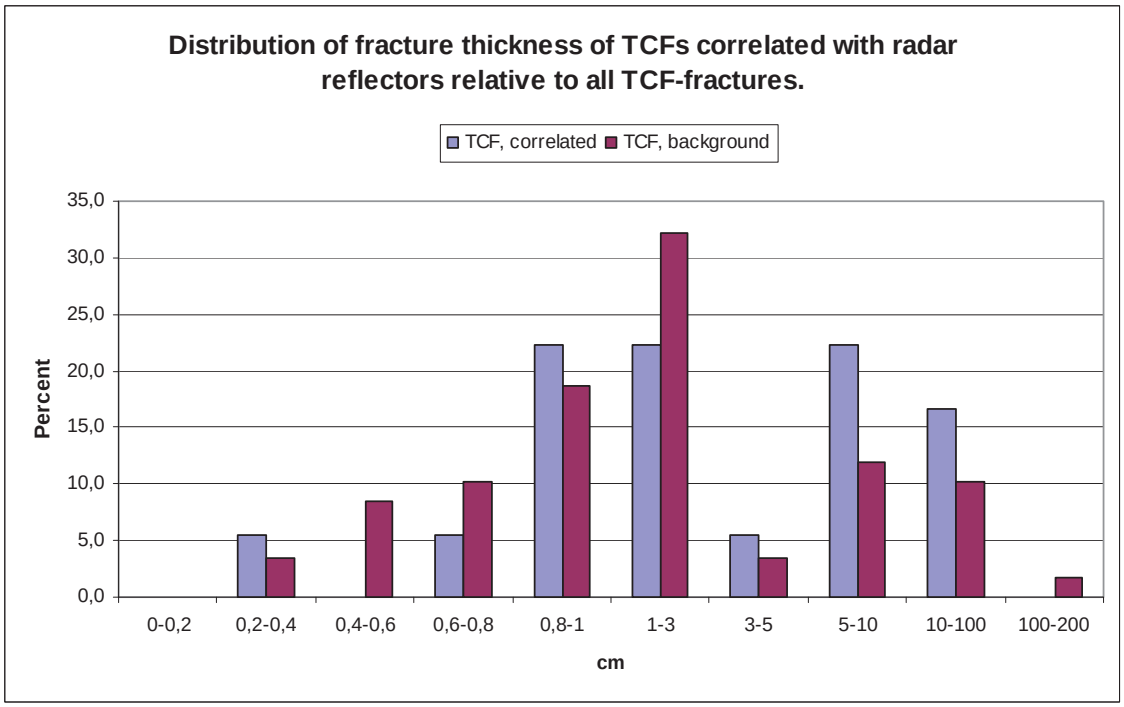

Figure 15. *Distribution of fracture filling thickness of TCFs correlated with radar reflector (n=18) compared to all TCFs within investigated tunnel sections (n=59).*

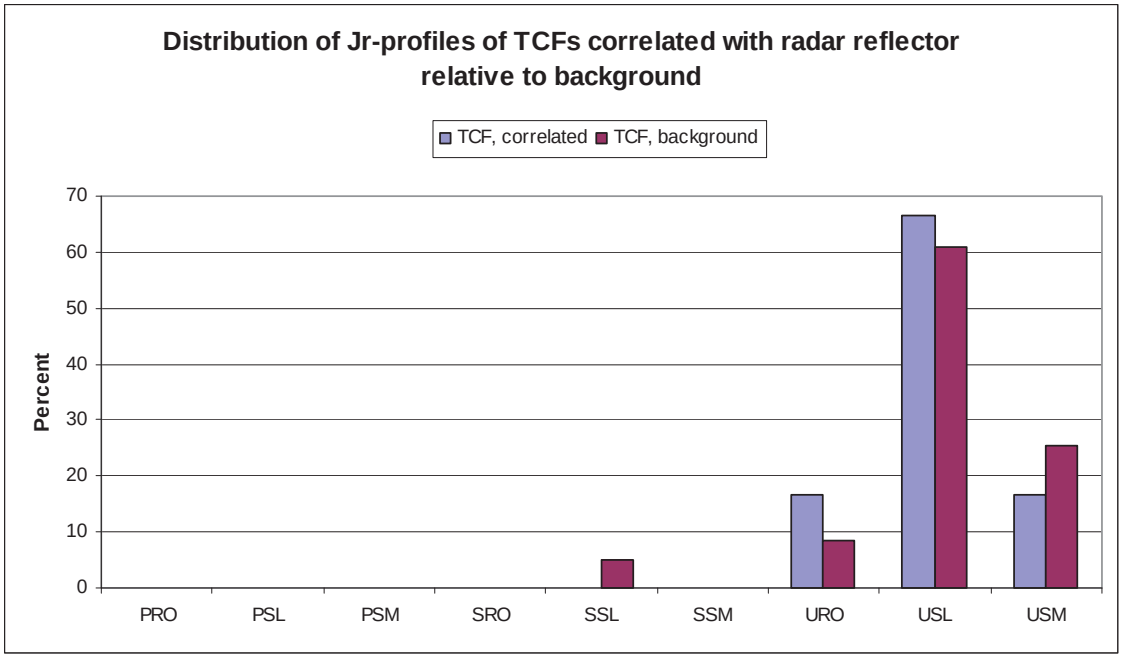

Figure 16. *Distribution of J_r-profiles of TCFs correlated with radar reflector (n=18) compared to all TCFs within investigated tunnel sections (n=59). PRO= Planar rough, PSL= Planar slickensided, PSM= Planar smooth, SRO= Stepped rough, SSL= Stepped slickensided, SSM= Stepped smooth, URO= Undulating rough, USL= Undulating slickensided, USM= Undulating smooth.*

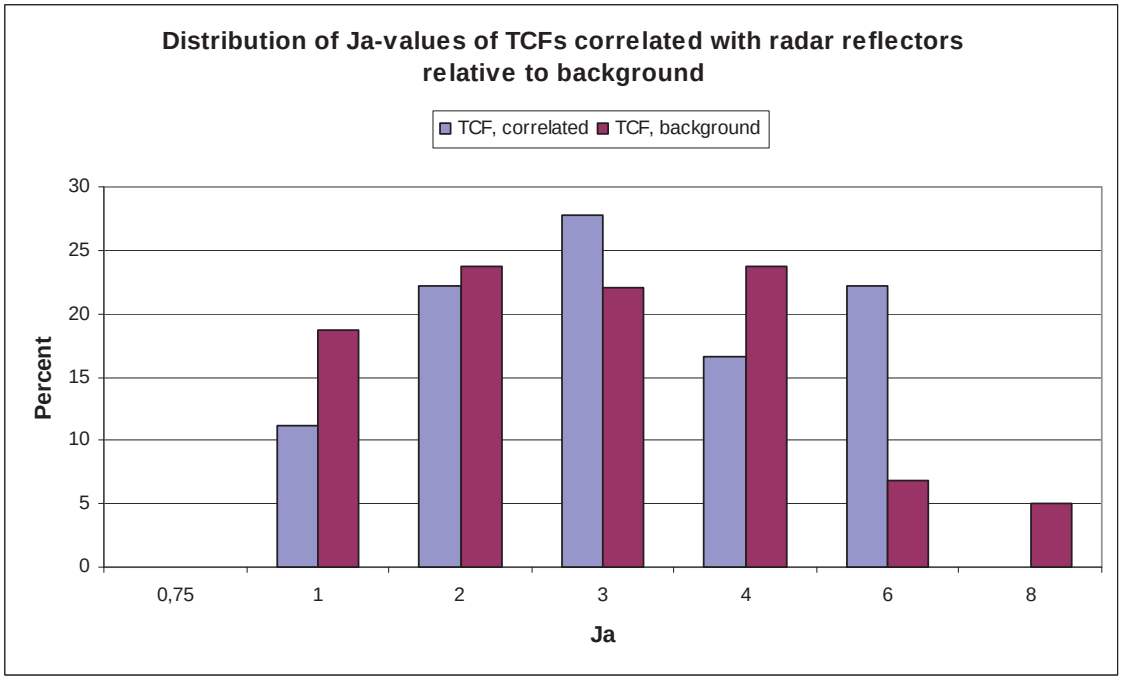

Figure 17. *Distribution of J_a-values of TCFs correlated with radar reflector (n=18) compared to all TCFs within investigated tunnel sections (n=59).*

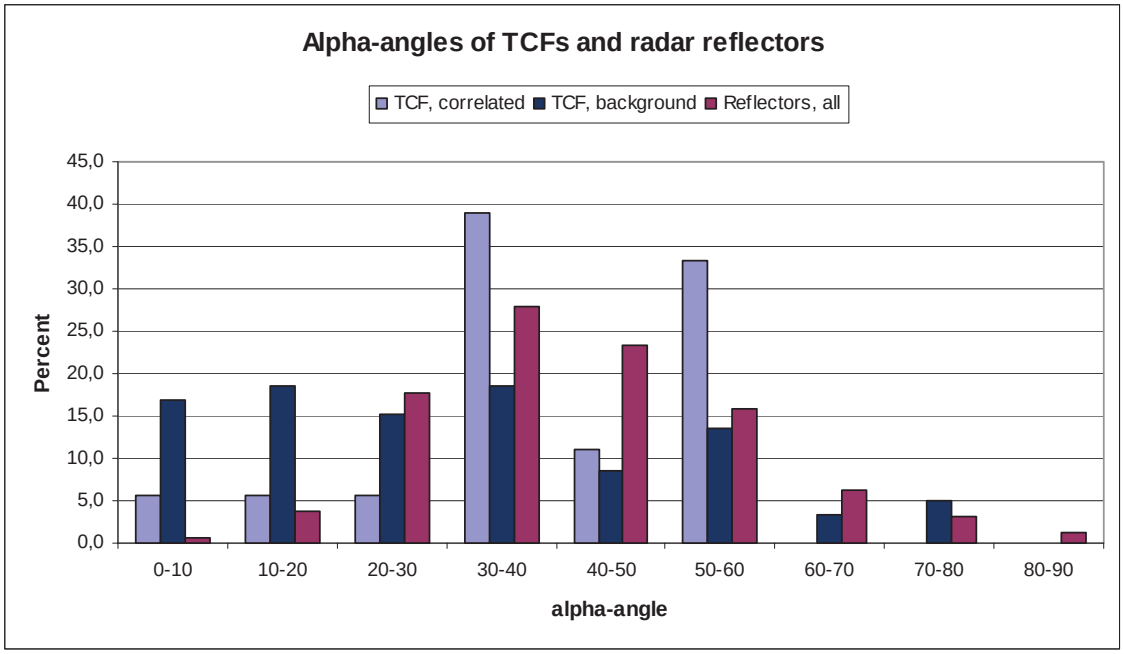

***Figure 18**. Alpha-angles of TCFs correlated with radar reflectors (n=18), all TCFs corresponding to pilot hole lengths (n=59) and all radar reflectors (n=158).*

Figure 18 showing alpha-angles of TCFs (both correlated TCFs and all TCFs in investigated tunnel sections) relative to alpha-angles of radar reflectors, clearly shows the low ability of radar to catch low angle structures, and that TCFs generally are low angle-structures. TCFs with alpha-angles of 30-60˚ are more easily correlated with radar reflectors than TCFs with alpha-angles of 0-30˚. The very few TCFs with alpha-angles of 60-90˚ could not be correlated with radar reflectors.

Since radar is sensitive to conductive material, water content in a fracture was thought to play a role in its visibility in radargrams. This study does not clearly support this hypothesis (Table 4), but on the other hand there were not many water conductive fractures in the investigated tunnel sections. Kinematic indicators, i.e. signs of movement in a fracture, does not either seem to enhance the visibility of the fracture in radargrams. No fracture zone type is either over- or underrepresented among the TCFs correlated with radar reflectors relative to other TCFs (Figure 19 and Table 5).

***Table 4.** Water content and kinematic indicators in TCFs correlated with radar reflectors relative to all TCFs within investigated tunnel sections.*

Property	**TCFs correlated with radar reflector**		**All TCFs within investigated tunnel sections**	
	no	**%**	**No**	**%**
Water content	3	16.7	6	10.20
Kinematic indicator, all	9	50.0	28	47.5
Kinematic indicator, certain	9	50.0	21	35.6
Number of TCFs	*18*		*59*	

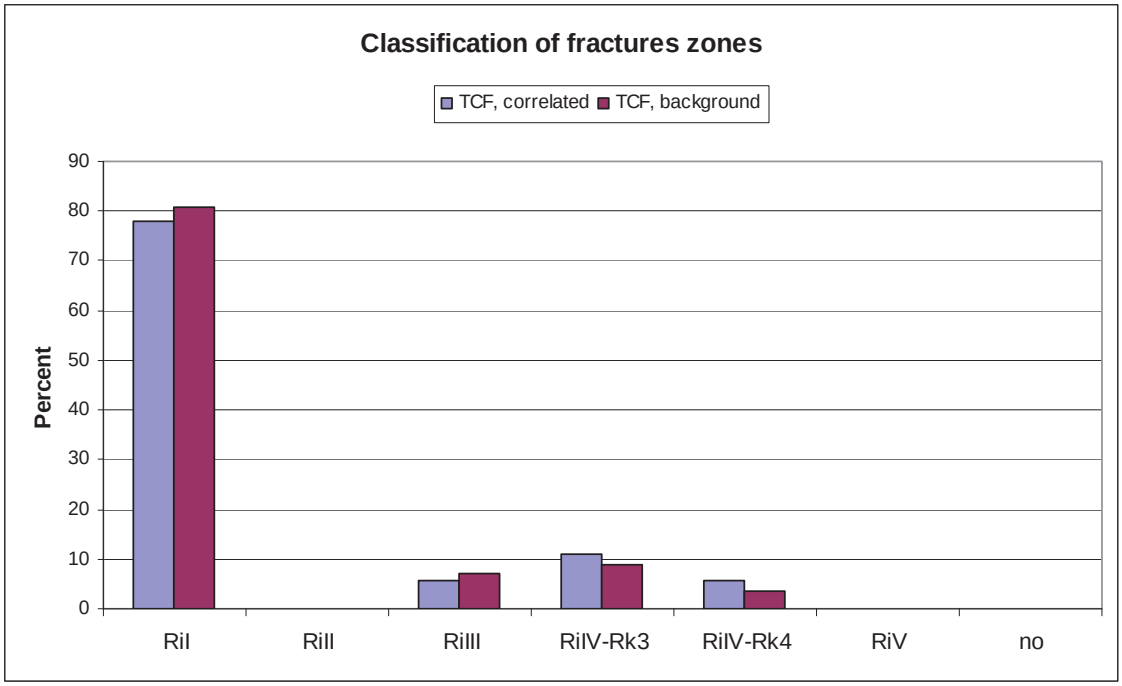

***Figure 19**. Distribution of fractures zone type of TCFs correlated with radar reflectors (n=18), relative to all TCFs corresponding to pilot hole lengths (n=57). For two TCF-fractures among the reference fractures Ri-classification is missing. Description of Ri-classes is found in Table 4-4.*

***Table 5.** Classification of fracture zones according to Gardemeister et al. (1976).*

Ri-Class	**Definition**
RiI	One or a few nearly planar fractures, with a length over 20 m or clearly continuing outside the tunnel.
RiII	Fractured section, where fracture spacing is 10-30 cm.
RiIII	Densely fractured section, where fracture spacing is less than 10cm.
RiIV-Rk3	Fractured section, where fracture spacing is 10-30 cm. Clay filled fractures.
RiIV-Rk4	Densely fractured section, where fracture spacing is less than 10 cm. Clay filled fractures.
RiV	Weak clay structure.

Almost all correlated TCFs are within stromatic or veined gneisses, while there are no correlated TCFs within diatexitic gneisses and K-feldspar porphyries (Figure 20). The one and only TCF within a pegmatitic granite was correlated with a radar reflector. Both stromatic and veined gneisses have a clear banded appearance. Bearing in mind that 2/3 of the reflectors correlated with TCFs also could be correlated with foliation it is still questionable whether these reflectors are a result of the TCFs or foliation.

The orientations of the correlated TCFs vary considerably and many of the correlated TCFs do not seem to belong to the main fracture sets (Figure A1-9).

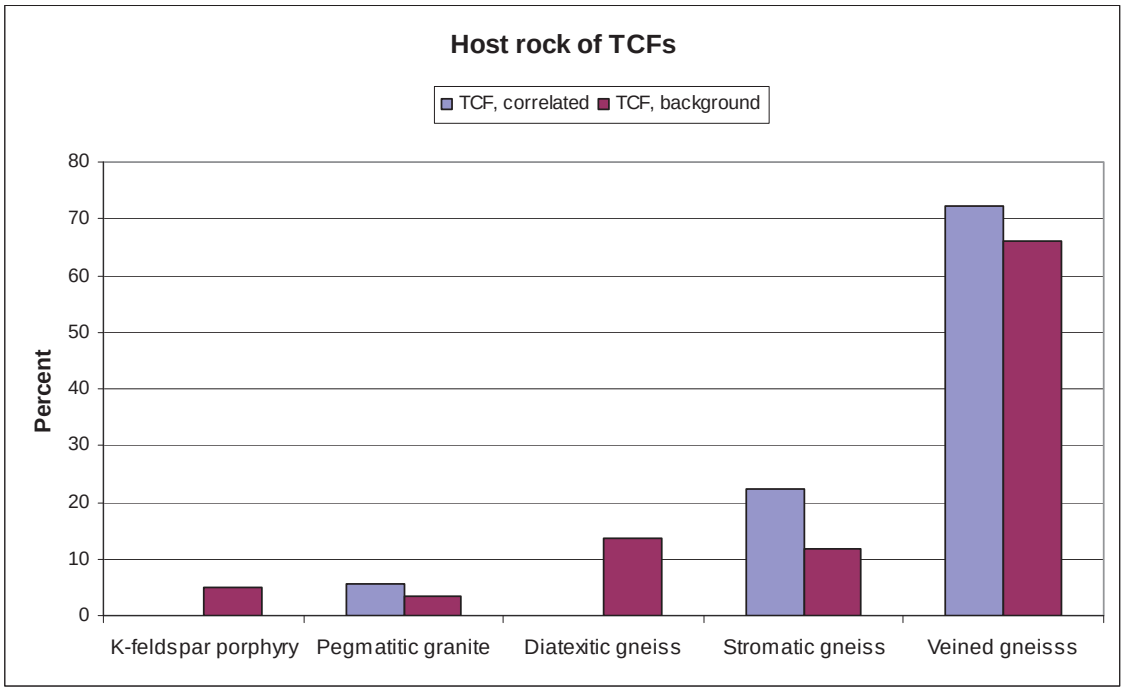

***Figure 20**. Distribution of host rock of TCFs correlated with radar reflectors (n=18), relative to all TCFs corresponding to pilot hole logging lengths (n=59).*

4 DISCUSSION AND CONCLUSION

The results of this study reveal the great difficulty of finding TCFs using pilot hole radar reflectors and pilot hole mapping data in a gneissic to migmatitic environment. Only 3 fractures of the 82 fractures (3.7 %) in the pilot holes that were correlated with radar reflectors were actually TCFs. Another 8 reflectors that were correlated with fractures could be explained by TCFs, although they were not correlated to the TCF itself. Using this method the probability of having an intersecting TCF in the pilot hole when the radar reflector is correlated with a fracture is about 10 %. To that, only 20 % of the TCFs are predicted.

When correlating the radar reflectors directly to TCFs in the tunnel, 18 TCFs or ~30 % of all TCFs could be correlated. Theoretically, the amount of predicted TCFs could be increased to these 30 % with the existing method. A great challenge is to pick the rough 10% of the reflectors that can be explained by TCFs. The author believes there are better ways to predict TCFs, which is discussed further down in this chapter.

Most TCFs lie with a low angle to the tunnel and the pilot hole. However, only a few low angle reflectors were identified. One possible explanation for this is that the disturbing ringing caused by the pilot hole fluid is filtered when processing the radar data, which in turns aggravates the possibility to identify low-angle reflectors. TCFs having an intersection angle of 70˚-90˚ are also less likely to be detected in radargrams. This means that a preferable intersection angle, being 30˚-60˚, is of importance for the visibility of TCFs in the radargram and it also explains why many TCFs are not caught by radar.

Another obstacle is the banding of the gneisses, which results in several reflectors. Only ~10 % of all reflectors do match a TCF and as many as 2/3 of the correlated TCFs could also be explained by foliation or the banding of the rock. This greatly affects the reliability of the results. Having a glimpse at the measured foliation orientations in the pilot hole, it seems that in most cases when both a TCF and the foliation could explain the reflector, the TCF and the foliation are not parallel. With further investigations it would be possible to sort out whether it is the foliation or the TCF that do cause the reflector. For this, the author suggests ground penetrating radar measurements with shielded 250 MHz antenna on the walls and roof of the tunnel. On the other hand, the reflector may also be a result of both a TCF and the foliation, since they have similar alpha-angle and the dipole antenna radiate and receive reflected signals from a 360-degree space (omnidirectionally).

Reinterpreting the radar data searching for reflectors in the intervals where TCFs occur, could also be interesting. How many reflectors that possibly could be correlated with TCFs were missed in the interpretation of radar data? Can the processing and interpretation of radar data be improved? Radar loggings with a 60 MHz directional antenna could also be interesting to test, since the reflectors are oriented (strike and dip revealed) and it has a longer penetration. The resolution is on the other hand poorer.

There seem to be better ways than radar alone to predict TCFs in pilot holes. By comparing the histograms showing pilot hole fracture properties and histograms showing TCF properties, as well as the stereographic projections, some conclusions can be made. It is likely that the fracture is a TCF if:

- the orientation is horizontal to sub-horizontal or vertical trending N-S.
- the width of the fracture $\geq$ 0.8 mm.
- J_a is $\geq$ 3.
- the fracture is slickensided.
- it contains in addition to calcite (~98 %) and chlorite (~83 %), also pyrite (~64 %), kaolinite (~53 %), graphite (~34 %), illite (~31 %), quartz (~25 %) and/or epidote (~15 %). Approximate probability of respective mineral occurrence in TCFs is in parenthesis. Of the mentioned minerals, quartz, graphite and epidote are clearly overrepresented in TCFs relative to background, since they are generally rare in other fractures.

Note that the difference in roughness in the histograms is related to scale rather than real difference in properties, for example: an observed undulating fracture in the tunnel may have a planar appearance in the pilot hole.

How well do the properties of radar reflectors match the typical TCF properties mentioned above?

- The horizontal to sub-horizontal TCFs are not very likely to be caught by radar due to their low angle to the pilot hole, while the vertical N-S trending set has a preferable alpha-angle.
- There is perhaps a slight overrepresentation of fractures with greater thickness and higher J_a-value among the fractures correlated with radar reflectors relative to all fractures, but slickensided fractures are not clearly overrepresented.
- When it comes to fracture minerals, both quartz and graphite are overrepresented in TCFs correlated with radar reflectors. Graphite is a conductive mineral which theoretically should result in radar reflectors.

After the completion of this study, the author’s conclusion is that radar should not be dismissed, but one must be very careful in interpreting radar data. Earlier work with identification of TCFs by analyzing geophysical data on pilot hole ONK-PH10 has shown some progress in finding TCFs (Heikkinen et al. 2011). In this work a radar reflector is only one anomaly amongst others, and perhaps it is as such it should be treated.

REFERENCES

Aalto, P., ed., Kosunen, P., Lahti, M., Pere, T., Tarvainen, A-M., Toropainen, V., Pekkanen, J. & Pöllänen, J. 2011a. Drilling and the Associated Drillhole Measurements of the Pilot Hole ONK-PH13. Posiva Oy. Working Report 2011-28.

Aalto & al., 2011b. Drilling and the Associated Drillhole Measurements of the Pilot Hole ONK-PH14. Posiva Oy. Working Report in progress.

Aaltonen Ismo (ed.), Lahti Mari, Posiva Oy, Engström Jon, Mattila Jussi, Paananen Markku, Paulamäki Seppo, Gehör Seppo, Kärki Aulis, Ahokas Turo, Torvela Taija, Front Kai. 2010. Geological Model of the Olkiluoto Site - version 2.0. Posiva Working Report 2010-70

Barton, N., 2002: Some new Q-value correlations to assist in site characterisation and tunnel design. International Journal of Rock Mechanics and Mining Sciences, Vol 39 (2002), pp 185-216.

Carlsten S. 2004. Oskarshamn site investigation - Geological interpretation of borehole radar reflectors in KSH01, HSH01–03, KAV01 and KSH02. SKB P-04-218, Svensk Kärnbränslehantering AB.

Carlsten S., Stanfors R., Askling P. and Annertz K. 1995. Comparison between borehole radar data and geological parameters from tunnel mapping. Measurements in cored boreholes during pre-investigation for Äspö. SKB PR 25-95-22, Svensk Kärnbränslehantering AB.

Döse C & Carlsten S., 2011: Investigation for identification of potential geological signatures for geophysical objects. SKB P-11-34. Svensk Kärnbränslehantering AB.

Engström, J. & Kemppainen, K., 2008. Evaluation of the Geological and Geotechnical Mapping Procedures in use in the ONKALO Access Tunnel. Posiva Oy. Working Report 2008-77.

Gardemeister, R., Johansson, S., Korhonen, P., Patrikainen, P. & Vähäsarja, P., 1976: Rakennusgeologisen kalliotutkimuksen soveltaminen. (The application of engineering geological bedrock investigation, in Finnish). Espoo: Technical Research Centre of Finland, Geotechnical laboratory. 38 p. Research note 25.

Heikkinen, E., Heinonen, S. & Ravimo, I. 2011. Semi-automated fracture classification procedure based on geophysical drill hole logging data. Posiva Oy. Working Report in progress.

Hellä, P. (ed), Ikonen, A., Mattila, J., Torvela, T., Wikström, L. 2009. RSC-Programme – Interim report. Approach and Basis for RSC development, Layout Determining Features and Preliminary Criteria for Tunnel and Deposition Hole Scale. Posiva Oy. Working Report 2009-29. 118 p.

Joutsen, Antti 2011. The use of geological data from pilot holes for predicting large fractures. Posiva Oy. Working Report in progress.

Kärki, A., Paulamäki, S. 2006. Petrology of Olkiluoto. Posiva report 2006-02. Posiva Oy, Eurajoki. 77 p.

Karttunen, P. (ed), Kemppainen, K., Kosunen, P., Lamminmäki, T., Lampinen, H., Pöllänen, J., Rautio, T. & Tarviainen, A-M., 2009. Drilling and the Associated Drillhole Measurements of the Pilot Hole ONK-PH8. Posiva Oy. Working Report 2009-16. 134 p.

Karttunen, P. (ed), Kosunen, P., Lamminmäki, T., Pekkanen, J., Pöllänen, J. & Tarviainen, A-M., 2010. Drilling and the Associated Drillhole Measurements of the Pilot Hole ONK-PH9. Posiva Oy. Working Report 2010-09. 194 p.

Karttunen, P., Mancini, P. (eds), Kasa, S., Pekkanen, J., Pere, T., Pöllänen, J., Tarvainen, A-M. & Toropainen, V., 2011. Drilling and the Associated Drillhole Measurements of the Pilot Hole ONK-PH11. Posiva Oy. Working Report 2011-03. 174 p.

Lahti, M. (ed), Käpyaho, E., Pekkanen, J., Pere, T., Pöllänen, J., Tarvainen, A-M. & Toropainen, V., 2011. Drilling and the Associated Drillhole Measurements of the Pilot Hole ONK-PH12. Posiva Oy. Working Report 2011-02. 148 p.

Lahti, M. (ed.), Ahokas, T., Nordbäck, N., Paananen M., Paulamäki, S., Vaittinen, T. 2009. The ONKALO Area Model. Version 1.1. Posiva working report 2009-113.

Mancini, P., Karttunen, P., Lokkila, M. (eds), Lamminmäki, T., Pekkanen, J., Pöllänen, J., Tarvainen, A-M., Toropainen, V., Kosunen, P. & Pere, T., 2011. Drilling and the Associated Drillhole Measurements of the Pilot Hole ONK-PH10. Posiva Oy. Working Report 2010-21. 176 p.

Munier, R. 2006. Using observations in deposition tunnels to avoid intersections with critical fractures in deposition holes. SKB R-06-54, Svensk Kärnbränslehantering AB (SKB) Stockholm, Sweden.

Nordbäck, Nicklas 2011. Tunnel Croscutting Fractures (TCF) in ONKALO chainage 2300-3910. Posiva Oy. Working Report 2011-xx (in review).

Olsson O. 1992. Characterization ahead of the tunnel front by radar and seismic methods – a case history from the Äspö Hard Rock Laboratory. SKB PR 25-92-01, Svensk Kärnbränslehantering AB.

Posiva Oy 2006, TKS-2006, Nuclear Waste Management of the Olkiluoto and Loviisa Power Plants: Programme for Research, Development and Technical Design for 2007-2009. Posiva Oy, Eurajoki. 285 p.

Posiva, 2009. Posiva Site Description 2008. Posiva Oy. POSIVA 2009-1.

Posiva Oy 2011. Olkiluoto Site Description 2011. Posiva Oy, Eurajoki. In Print.

Saksa, P., Hellä, P., Lehtimäki, T., Heikkinen, E. & Karanko, A. 2001. Reikätutkan toimivuusselvitys (Investigation of the performance of drill hole radar, *in Finnish*). Posiva, Working Report 2001-35, 134 p.

SKB, 1994. Supplementary investigations of fracture zones in the tunnel, core mapping and radar measurement – Compilation of technical notes – Measurements performed during construction of section 1475-2265 m. SKB PR 25-94-01. Svensk Kärnbränslehantering AB.

SKB, 1995. Passage through water bearing fracture zones – Compilation of technical notes – Passage through fracture zone NE-1m. Geology and geophysics. PR 25-95-18b. Äspölaboratoriet.

Stenberg L. and Forslund O. 1996. Results of GPR radar measurements at Zedex site, Äspö, Sweden. SKB PR HRL-96-06, Svensk Kärnbränslehantering AB.

Stephens M. and Skagius K. Ed., 2007. Geology - Background complementary studies. Forsmark stage modelling 2.2. SKB R-07-56, Svensk Kärnbränslehantering AB.

Vaittinen, T., Ahokas, H. & Nummela, J., 2009. Hydrogeological structure model of the Olkiluoto Site – update in 2008. Posiva working report 2009-15.

APPENDIX 1. STEREOGRAPHIC PROJECTIONS SHOWING FRACTURES CORRELATED WITH PILOT HOLE RADAR REFLECTORS IN RELATION TO MAIN FRACTURE SETS

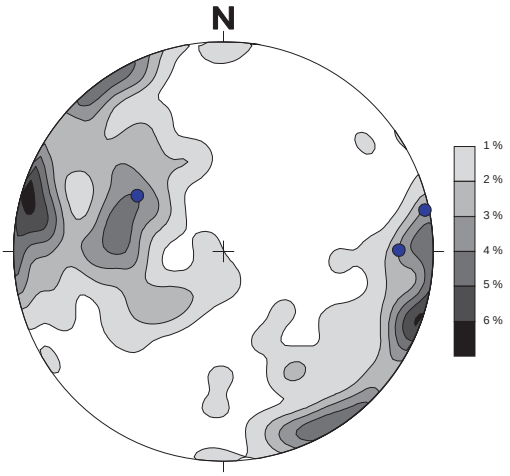

***Figure A1-1**: Contoured fracture orientations (n= 154) in ONK-PH8. Fractures correlated with radar reflectors (●, n=3) in ONK-PH8.*

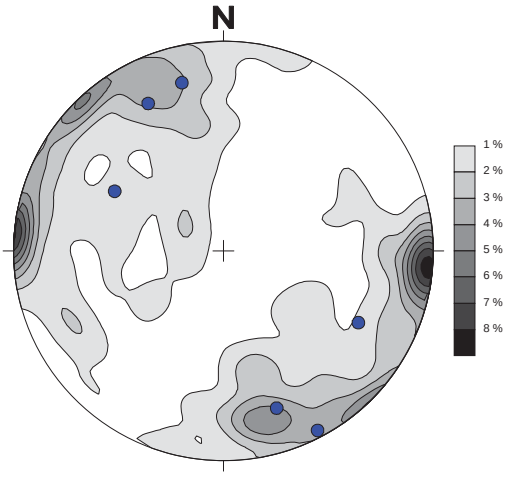

***Figure A1-2**: Contoured fracture orientations (n= 269) in ONK-PH9. Fractures correlated with radar reflectors (●, n=6, for one fracture dip and dip direction-values are missing) in ONK-PH9.*

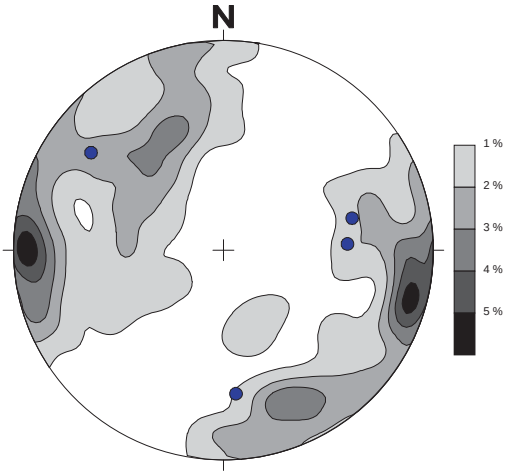

Figure A1-3: *Contoured fracture orientations (n= 337) in ONK-PH10. Fractures correlated with radar reflectors (●, n=4) in ONK-PH10.*

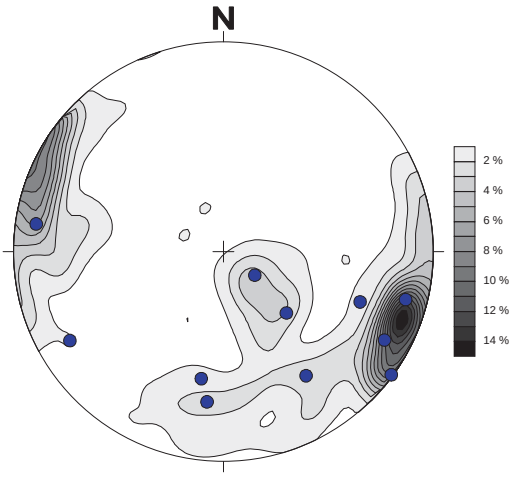

Figure A1-4: *Contoured fracture orientations (n= 190) in ONK-PH11. Fractures correlated with radar reflectors (●, n=11) in ONK-PH11.*

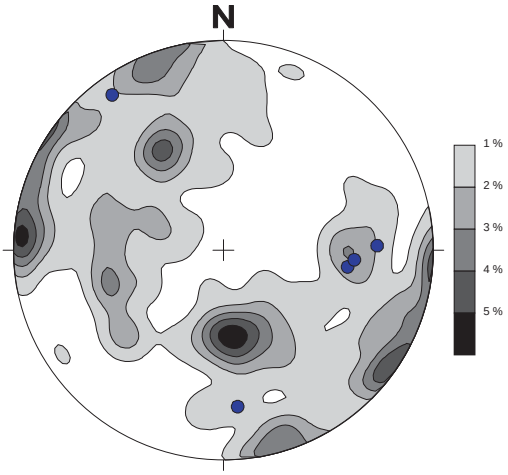

Figure A1-5: *Contoured fracture orientations (n= 164) in ONK-PH12. Fractures correlated with radar reflectors (●, n=5) in ONK-PH12*

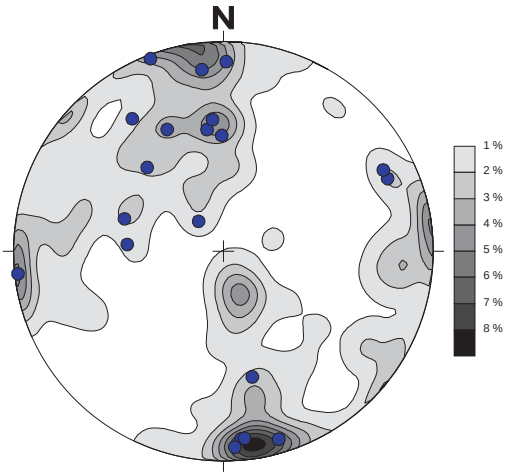

Figure A1-6: *Contoured fracture orientations (n= 152) in ONK-PH13. Fractures correlated with radar reflectors (●, n=20) in ONK-PH13.*

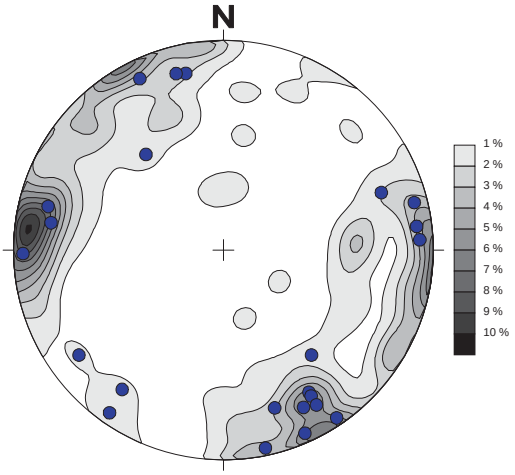

Figure A1-7: *Contoured fracture orientations (n= 148) in ONK-PH14. Fractures correlated with radar reflectors (●, n=23) in ONK-PH14.*

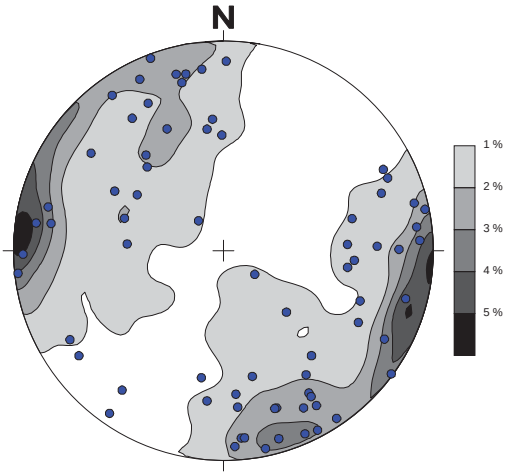

Figure A1-8: *Contoured fracture orientations (n= 1414) in pilot holes ONK-PH8-14. Fractures in pilot holes ONK-PH8-14 that are correlated with radar reflectors (●, n=72).*

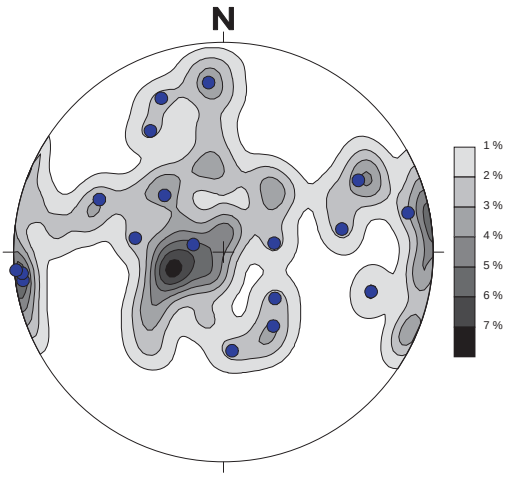

***Figure A1-9**: Contoured fracture orientations of all TCFs (n= 59) within investigated tunnel sections. TCFs correlated with radar reflectors (●, n=18).*

APPENDIX 2. RADAR REFLECTORS VERSUS TCF

Radar interpretation						Correlated structure in pilot hole	Correlated TCF (Tunnel mapping data)						
Borehole	Name	Depth	Corresponding tunnel length	alpha-angle	Comment reflector		Fracture Nr REFERENCE	Fracture Nr (mapping)	Chainage	~alpha-angle	dip	dip dir.	Correlation
ONK-PH8		11,45	3127,5	71			P319	3120_9	3125-3127	60	54	113	Good
ONK-PH8		31,28	3147,3	49		fracture	P321	3150_1	3148-3152	40	37	140	Acceptable
ONK-PH8		32,45	3148,5	59			no						
ONK-PH8		39,12	3155,1	52	possibly smaller alpha angle	foliation	P322	3150_3	3154-3157	37	32	134	Good
ONK-PH8		57,37	3173,4	44		fracture	no						
ONK-PH8		83,26	3199,3	46			no						
ONK-PH8		83,93	3199,9	48		fracture	no						
ONK-PH8	1	95,78	3211,8	52			no						
ONK-PH9	1	26,84	3289,8	64		fracture							
ONK-PH9	2	47,25	3310,3	50		fracture							
ONK-PH9	3	55,60	3318,6	90									
ONK-PH9	4	64,00	3327,0	90									
ONK-PH9	5	78,01	3341,0	56		fracture	P336	3335_22	3338-3350	54	62	285	Good
ONK-PH9	6	83,89	3346,9	49		fracture	P336	3335_22	3338-3350	54	62	285	Acceptable
ONK-PH9	7	86,60	3349,6	55		fracture/ foliation	P338	3350_1	3350-3352	54	86	82	Good
ONK-PH9	8	89,13	3352,1	53		fracture/ foliation	P338	3350_1	3350-3352	54	86	82	Good
ONK-PH9	9	90,65	3353,7	44		fracture							
ONK-PH9	10	118,99	3382,0	32									
ONK-PH10	L-9	9,03	3468,0	61		foliation	no						
ONK-PH10	L-1	33,33	3492,3	47		foliation	no						
ONK-PH10	L-2	53,52	3512,5	65		foliation	P350	3510_4	3510	51	57	149	Good
ONK-PH10	L-3	54,62	3513,6	69		fracture	no						
ONK-PH10	L-4	63,08	3522,1	65		fracture	no						
ONK-PH10	L-5	67,67	3526,7	55		foliation	no						
ONK-PH10	L-6	68,18	3527,2	55		foliation	no						
ONK-PH10	L-7	71,83	3530,8	77		fracture	no						
ONK-PH10	L-8	72,56	3531,6	73		fracture	no						
ONK-PH11	L-3	8,43	3930,4	26		fracture	no						
ONK-PH11	L-15	10,64	3932,6	55		fracture	no						
ONK-PH11	L-16	12,99	3935,0	60		fracture	no						
ONK-PH11	L14	25,43	3947,4	60		fracture	no						
ONK-PH11	L-4	30,90	3952,9	20		fracture	no						
ONK-PH11	L-10	56,77	3978,8	50		fracture	no						
ONK-PH11	L-13	60,42	3982,4	65		fracture	no						
ONK-PH11	L-1	70,12	3992,1	22		fracture	no						
ONK-PH11	L-2	73,76	3995,8	24		fracture/ foliation	P362	3995_1	3995	33	27	312	Good
ONK-PH11	L-5	81,05	4003,1	40		fracture	P363	4000_23	4003	31	39	355	Good
ONK-PH11	L-9	102,18	4024,2	55		fracture	no						
ONK-PH11	L-8	117,32	4039,3	20		foliation	no						
ONK-PH11	L-14	9,13	4101,1	25		foliation	no						
ONK-PH12	L-12	15,60	4107,6	26		foliation	P370	4110_8	4110	25	35	99	Good
ONK-PH12	L-13	17,11	4109,1	27		foliation	same as above?						
ONK-PH12	L-10	22,51	4114,5	33		fracture	no						
ONK-PH12	L-11	24,00	4116,0	34		foliation	no						

Radar interpretation						Correlated	Correlated TCF (Tunnel mapping data)						
Borehole	Name	Depth	Corresponding tunnel length	alpha-angle	Comment reflector	structure in pilot hole	Fracture Nr REFERENCE	Fracture Nr (mapping)	Chainage	~alpha-angle	dip	dip dir.	Correlation
ONK-PH12	L-9	48,27	4140,3	25		foliation	no						
ONK-PH12	L-8	63,69	4155,7	61		fracture	no						
ONK-PH12	L-6	84,35	4176,4	44		fracture	P372	4170_3	4178	36	48	259	Good
ONK-PH12	L-5	93,61	4185,6	35		fracture/ foliation	P375	4180_4	4183	27	62	242	Good
ONK-PH12	L-7	94,57	4186,6	9			P378	4185_13	4190	7	12	104	Very good
ONK-PH12	L-4	95,88	4187,9	38		fracture	P376	4180_6	4086	27	50	245	Acceptable
ONK-PH12	L-3	105,87	4197,9	42		foliation	no						
ONK-PH12	L-2	110,41	4202,4	59	same as Ph13, L2		no						
ONK-PH12	L-1	123,13	4215,1	41	same as PH13, L4		no						
ONK-PH13	L-27-inclined-wall	-2,02	4199,0	25			no						
ONK-PH13	L-2-TunnelWall	-0,46	4200,5	57	same as PH12, L-2		no						
ONK-PH13	L-3-moderate-at-6m	6,42	4207,4	33		foliation	no						
ONK-PH13	L-4-moderate-at-15m	14,95	4216,0	35	same as PH12, L-1	foliation	no						
ONK-PH13	"L36" gentle	18,80	4219,8	32		foliation	no						
ONK-PH13	L-26-moderate	19,50	4220,5	80			no						
ONK-PH13	L-25-moderate	23,47	4224,5	32		fracture	no						
ONK-PH13	L-32_inclined	27,12	4228,1	12			P380	4205_7	4210	12	33	224	Poor
ONK-PH13	L-5-distinct-31m	29,80	4230,8	21		fracture	P381	4230_7	4237	32	78	176	Poor
ONK-PH13	L-24_inclined_upwds	38,24	4239,2	20		fracture	P382	4240_8	4244	16	38	175	Acceptable
ONK-PH13	L-6-strong-44m	44,63	4245,6	28		fracture	no						
ONK-PH13	L-7-strong-52m	52,48	4253,5	35		fracture	no						
ONK-PH13	L7 lower	56,00	4257,0	20		foliation	no						
ONK-PH13	L-8-strong-60m	59,36	4260,4	32		fracture	no						
ONK-PH13	L-23-short-conduc	61,94	4262,9	48		fracture	no						
ONK-PH13	L-22-short-conduc	66,96	4268,0	60			no						
ONK-PH13	L-21-short	73,12	4274,1	34		fracture	no						
ONK-PH13	L-20-short-conduc	77,99	4279,0	28		fracture/ foliation	P383	4280_1	4280	31	70	175	Very good
ONK-PH13	L-19-short-81	80,98	4282,0	52		fracture	no						
ONK-PH13	L-33_add_zone_	84,70	4285,7	47		fracture	no						
ONK-PH13	L-18-short-cond-stron	87,84	4288,8	45		fracture	no						
ONK-PH13	"L35" added from excel	90,10	4291,1	55		fracture	no						
ONK-PH13	L-9_conductor_95m	93,72	4294,7	46		fracture	no						
ONK-PH13	L-17-short-strong	98,00	4299,0	51			no						
ONK-PH13	L-16-str-short	99,56	4300,6	33		fracture	no						
ONK-PH13	L-1-TGG-contact	103,66	4304,7	41			no						
ONK-PH13	L-13-str111-noreachbh	110,31	4311,3	22		fracture	no						
ONK-PH13	L-15-weak-in-tgg	113,55	4314,6	39		fracture	no						
ONK-PH13	L-34new117	116,58	4317,6	41		fracture	no						
ONK-PH13	L-29-at113out-of-bh	120,77	4321,8	36			no						
ONK-PH13	L-12-short-at-123m	121,92	4322,9	54			no						
ONK-PH13	L-14-angle18at115mpt	122,84	4323,8	18			no						
ONK-PH13	L-31-short	126,53	4327,5	47			no						
ONK-PH13	L-11-strong-wavy	128,07	4329,1	26			P387	4330_1		20	20	260	Good
ONK-PH13	L-28-130m-inclined	128,73	4329,7	36			no						
ONK-PH13	L-30-short	131,54	4332,5	48	as PH14, L9	fracture/ foliation?	P386	4330_17		53	86	84	Very good

Radar interpretation						Correlated	Correlated TCF (Tunnel mapping data)						
Borehole	Name	Depth	Corresponding tunnel length	alpha-angle	Comment reflector	structure in pilot hole	Fracture Nr REFERENCE	Fracture Nr (mapping)	Chainage	~alpha-angle	dip	dip dir.	Correlation
ONK-PH13	L-10-strong_end_of_BH	136,96	4338,0	33		fracture	no						
ONK-PH14	L-2	-3,44	4309,6	41	same as PH13, L1???		P385	4305_5	4310	56	69	98	Acceptable
ONK-PH14	L-3	-0,44	4312,6	28	same as PH13, L13?		no						
ONK-PH14	L-1	0,56	4313,6	42	same as PH13, L15?	fracture	no						
ONK-PH14	L-4	5,35	4318,3	24		fracture	no						
ONK-PH14	L-5	9,94	4322,9	69	same as PH13, L12?	fracture	no						
ONK-PH14	L-6	13,29	4326,3	33		foliation	no						
ONK-PH14	L-7	14,44	4327,4	33		foliation	no						
ONK-PH14	L-8	16,06	4329,1	35		foliation	no						
ONK-PH14	L-9	17,69	4330,7	45	same as PH13, L30?	foliation	P386	4330_17		53	86	84	Good
ONK-PH14	L-10	21,61	4334,6	26		fracture	P387	4330_1		20	20	260	Acceptable
ONK-PH14	L-12	22,76	4335,8	40		foliation	no						
ONK-PH14	L-11	23,53	4336,5	27		fracture	no						
ONK-PH14	L-13	24,29	4337,3	41		fracture	no						
ONK-PH14	L-14	25,82	4338,8	36	same as PH13, L10?	fracture	no						
ONK-PH14	L-15	28,46	4341,5	35		fracture	no						
ONK-PH14	L-19	30,23	4343,2	23			P388	4340_9		11	24	226	Acceptable
ONK-PH14	L-16	30,32	4343,3	40		fracture	no						
ONK-PH14	L-17	31,81	4344,8	41		fracture	no						
ONK-PH14	L-18	33,29	4346,3	40		fracture	no						
ONK-PH14	L-22	36,45	4349,4	36		foliation	no						
ONK-PH14	L-56B	37,88	4350,9	46		fracture	no						
ONK-PH14	L-20	38,36	4351,4	38			no						
ONK-PH14	L-24	39,80	4352,8	37		foliation	no						
ONK-PH14	L-23	43,62	4356,6	32		foliation	no						
ONK-PH14	L-36	46,21	4359,2	29		foliation	no						
ONK-PH14	L-27	47,26	4360,3	39		foliation	P389	4355_16		44	68	158	Good
ONK-PH14	L-25	48,41	4361,4	36		foliation	no						
ONK-PH14	L-26	50,13	4363,1	39		foliation	no						
ONK-PH14	L-28	51,28	4364,3	40		foliation	no						
ONK-PH14	L-55B	53,03	4366,0	50		fracture	P390	4365_1		48	79	258	Very good
ONK-PH14	L-29	53,23	4366,2	18		fracture/ foliation	no						
ONK-PH14	L-21	54,22	4367,2	47		fracture	no						
ONK-PH14	L-30	54,61	4367,6	32		fracture	no						
ONK-PH14	L-57B	58,65	4371,7	37		foliation	no						
ONK-PH14	L-32	62,89	4375,9	29		foliation	no						
ONK-PH14	L-33	68,02	4381,0	49		fracture	no						
ONK-PH14	L-34	69,99	4383,0	50		fracture/ foliation	P391	4380_1		55	89	85	Very good
ONK-PH14	L-35	70,05	4383,1	28		fracture	no						
ONK-PH14	L-66	71,96	4385,0	30		fracture	no						
ONK-PH14	L-37	75,32	4388,3	40		fracture	no						
ONK-PH14	L-38	80,84	4393,8	45		fracture	no						
ONK-PH14	L-40	83,40	4396,4	27		foliation	no						
ONK-PH14	L-39	85,37	4398,4	29			no						

Radar interpretation						Correlated	Correlated TCF (Tunnel mapping data)						
Borehole	Name	Depth	Corresponding tunnel length	alpha-angle	Comment reflector	structure in pilot hole	Fracture Nr REFERENCE	Fracture Nr (mapping)	Chainage	~alpha-angle	dip	dip dir.	Correlation
ONK-PH14	L-41	91,68	4404,7	36		foliation	no						
ONK-PH14	L-42	95,63	4408,6	45		fracture	no						
ONK-PH14	L-54B	96,61	4409,6	28		foliation	no						
ONK-PH14	L-43	98,59	4411,6	42		foliation	no						
ONK-PH14	L-53B	101,32	4414,3	36		fracture	no						
ONK-PH14	L-44	103,23	4416,2	50		foliation	no						
ONK-PH14	L-45	105,04	4418,0	40		foliation	no						
ONK-PH14	L-46	107,24	4420,2	40		fracture	no						
ONK-PH14	L-48	108,19	4421,2	28		foliation	no						
ONK-PH14	L-47	109,15	4422,1	34		foliation	no						
ONK-PH14	L-49	110,10	4423,1	42		foliation	no						
ONK-PH14	L-50	112,49	4425,5	72		fracture	no						
ONK-PH14	L-51	114,88	4427,9	21			no						
ONK-PH14	L-52	117,74	4430,7	56		fracture	no						
ONK-PH14	L-59	121,56	4434,6	49		fracture	no						
ONK-PH14	L-53	123,47	4436,5	45		fracture	no						
ONK-PH14	L-55	128,73	4441,7	51		fracture	no						
ONK-PH14	L-54	130,16	4443,2	38		foliation	P392	4440_8		36	35	326	Very good
ONK-PH14	L-56	131,11	4444,1	37		foliation	as above?						
ONK-PH14	L-58	138,75	4451,8	43		fracture	no						
ONK-PH14	L-57	142,09	4455,1	33		foliation	no						
ONK-PH14	L-60	144,96	4458,0	40		fracture	no						
ONK-PH14	L-61	146,87	4459,9	42		foliation	no						
ONK-PH14	L-62	150,29	4463,3	59		fracture	no						
ONK-PH14	L-63	152,29	4465,3	39			no						
ONK-PH14	L-65	156,79	4469,8				no						
ONK-PH14	L-64	158,79	4471,8				no						